Geophys. J. R. astr. Soc. (1975) **42**, 899–929.

Elasticity of Olivine (α), Beta(β), and Spinel (γ) Polymorphs of Germanates and Silicates

Robert C. Liebermann

(Received 1974 November 12)

Summary

Ultrasonic data for the velocities of germanate and silicate compounds in the olivine (α), beta (β) and spinel (γ) crystal structures have been determined as a function of pressure to 7·5 kbar at room temperature for polycrystalline specimens hot-pressed at pressures up to 65 kbar. The α–γ phase transformations are characterized by the following velocity (v)–density (ρ) relationships: (a) the velocity jumps are twice the percentage magnitude of the density jumps; (b) the ratio (v_P/v_s) of the compressional to shear velocity is either approximately constant or increases slightly across the transitions; and (c) the slopes (linear or logarithmic) on v–ρ diagrams for the α–γ transition are comparable to those produced by isothermal compression or isobaric expansion of the low-pressure olivine phase. The behaviour of v_P/v_s is a feature common to many phase transformations. However, the observed relationships (a) and (c), while similar to those for the quartz-coesite transition in SiO_2, are in marked contrast with those for the coesite-rutile, pyroxene-garnet and pyroxene-ilmenite transformations. These latter transitions involve increases in cation–anion co-ordination and nearest-neighbour distances whereas the olivine-spinel and olivine-beta phase transformations do not. Such crystallographic details may be diagnostic for interpretations of the composition and mineralogy of the Earth's transition zone. Systematic trends in the elastic properties for isostructural sequences support the concept of germanates as models for the elasticity of their silicate analogues; this scheme is applied to estimate the bulk modulus of the spinel polymorph of Mg_2SiO_4 ($K_s = 2{\cdot}06 \pm 0{\cdot}05$ Mbar). Comparison of the new elasticity data with recent Earth models in the vicinity of the 400-km discontinuity reveals that only model 1066B of Gilbert & Dziewonski is compatible with the experimental data for the α–γ and α–β transformations.

1. Introduction

Mineralogical investigations, notably in the laboratories of Ringwood and Akimoto, have demonstrated that orthosilicate olivines transform to the spinel or beta phase structures at elevated pressures and temperatures (reviewed by Ringwood & Major 1970; Akimoto 1972). These studies provide crystallographic data on the density variation across such polymorphic phase transformations. As the most directly observable parameters of the Earth's interior are the seismic wave velocities,

the usefulness to geophysics of these laboratory data would be greatly enhanced if measurements of the elastic properties of the high-pressure phases were available. The experimental difficulties involved in producing sufficient quantities of the high-pressure minerals to make acoustic measurements are formidable. Nevertheless, such data are so vital to geophysics that considerable efforts have been made to produce such specimens in these laboratories over the past few years (Mizutani *et al.* 1970; Mizutani, Hamano & Akimoto 1972; Akimoto 1972; Liebermann 1972b, 1973a, c, 1974; Liebermann & Ringwood 1973).

Concurrent with this progress in high-pressure mineralogy have been complementary developments in seismological studies of the velocity and density structure of the Earth's mantle. Sophisticated inversion techniques applied to gross Earth geophysical data (particularly, the eigenperiods of normal modes) have enabled direct determination of the density and velocity distribution with depth. Unfortunately, the normal mode data now available lack the resolving power to delineate the fine structure of the transition zone (350–1000 km) between the upper and the lower mantle, the region in which one would predict from laboratory data that the open-packed silicates of the upper mantle transform to more densely-packed crystal structures (reviewed by Ringwood 1970, 1975). Gilbert & Dziewonski (1975) have shown that both continuous (1066A) and discontinuous (1066B) functions for the velocity-depth and density-depth profiles in this region give equally good fits to the data. However, the combined weight of other seismic data from surface wave studies, $dT/d\Delta$ studies using large seismic arrays, travel times from explosions, detailed studies of wave forms, and precursors to the phase $P'P'$ support the likelihood of there being two major first-order discontinuities in those functions near 400 and 650 km depth (Jordan & Anderson 1974; Dziewonski, Hales & Lapwood 1975; Hales 1972 and private communication). It is the first of these discontinuities that has been associated with the transformation of $(Mg, Fe)_2SiO_4$ olivine to the spinel or beta phase structures since Bernal's (1936) suggestion was adopted by Jeffreys (1937) (reviewed by Ringwood 1970).

The ultrasonic programme in our laboratory to determine the elastic properties of the low- and high-pressure polymorphs of various compounds undergoing phase transformations may thus be viewed as providing the missing link in the chain connecting the high-pressure mineralogical studies to the geophysical models derived from seismological data. The purpose of this paper is to report the complete elasticity data for a number of germanate and silicate compounds in the olivine, spinel and beta phase structures, to discuss the importance of these data for velocity-density systematics proposed by other investigators, and to compare the laboratory data with geophysical models in the neighbourhood of the 400 km discontinuity. This paper augments and supplements the brief reports and discussions of these data which we have presented earlier (Liebermann 1972b, 1973a, b; Liebermann & Ringwood 1973).

2. Experimental procedure

2.1 *Specimen preparation*

Powder samples of eight chemical compounds were synthesized from the component oxides at atmospheric pressure (with the exception of Ni_2SiO_4 for which the Grade A quality powder was purchased from Tem Pres, Inc., State College, Pennsylvania, USA). Details of the sintering procedure are given in Table 1 as are the crystallographic structures of the synthesized powders. The composition and crystallographic structure of these powders were confirmed by optical examination and X-ray diffraction photographs. Polycrystalline specimens of the following germanates and silicates were then hot-pressed in piston-cylinder ($P < 35$ kbar) or girdle ($P < 60$ kbar) solid-media apparati: olivines—Mg_2GeO_4, $MgMnGeO_4$, Mn_2GeO_4,

Table 1

Details of preparation of hot-pressed polycrystalline specimens.

Compound	Structure	Starting material[1]			Hot-pressing conditions			Length	Density	
		Synthesis T °C	Time (hr)	Structure	P (kbar)	T (°C)	Time (hr)	(mm)	Bulk (g cm^{-3})	%X-ray
Mg_2GeO_4	Olivine (α)	1350	3	olivine	8	1200	1·5	4·061	3·97	98·3
$MgMnGeO_4$	Olivine (α)	1300	2	olivine	16	950	1	4·354	4·35	98·7
Mn_2GeO_4	Olivine (α)	1050	16	olivine[2]	15	850	0·75	2·921	4·72	98·5
Ni_2SiO_4	Olivine (α)	—	—	olivine[3]	15	1000	1	4·707	4·80	97·4
Mg_2GeO_4	Spinel (γ)	1350	3	olivine	35	1200	1·25	2·357	4·32	98·6
Fe_2GeO_4	Spinel (γ)	900	16	spinel[4]	30	840	1	3·713	5·46	98·6
Co_2GeO_4	Spinel (γ)	1250	3	spinel	30	1000	1	3·414	5·81	98·9
Ni_2GeO_4	Spinel (γ)	1300	3	spinel	30	1000	1	1·605	6·02	99·1
Ni_2SiO_4	Spinel (γ)	—	—	olivine[3]	56	1100	1·5	2·126	5·12	95·7
Fe_2SiO_4	Spinel (γ)	900	16	olivine[5]	58	1000	2	2·040	4·68	96·5
Mn_2GeO_4	beta (β) phase	1050	16	olivine[2]	52	1000	1·5	1·867	5·03	97·9

[1] Unless otherwise stated, compounds synthesized by mixing component oxides and sintering in air at atmospheric pressure.

[2] Mix sealed in evacuated SiO_2 tube with Fe buffer.

[3] Tem-Pres. grade A powder dried for 1 h at 1100 °C.

[4] Mix Fe_2O_3 and Fe with GeO_2, wrap in Pt foil, and seal in evacuated SiO_2 tube.

[5] Mix Fe_2O_3 and SiO_2 and sinter at 1050 °C for 3 h, then crush and mix in Fe metal, pelletize and place in Fe bucket and seal in evacuated SiO_2 tube and heat at 900 °C overnight.

Table 2

Lattice parameters, molar volumes and densities of germanate and silicate compounds with olivine, spinel and beta phase crystal structures.

Compound	Structure	Lattice parameters a	b	c	Z (molecules/unit cell)	Molar volume (cc/mole)	Molar weight (g)	Density ($g\,cm^{-3}$)	Reference
			Å						
Mg_2GeO_4	(α) orthorhombic	4·915	10·295	6·020	4	45·87	185·21	4·038	Dachille & Roy (1960)
$MgMnGeO_4$	(α) orthorhombic	4·982	10·559	6·181	4	48·96	215·84	4·408	Ringwood & Reid (1970)
Mn_2GeO_4	(α) orthorhombic	5·061	10·719	6·295	4	51·42	246·46	4·793	Morimoto *et al.* (1969)
Ni_2SiO_4	(α) orthorhombic	4·721	10·119	5·910	4	42·51	209·50	4·928	Akimoto, Fujisawa & Katsura (1965)
Mg_2GeO_4	(γ) cubic	8·255	—	—	8	42·35	185·21	4·373	Dachille & Roy (1960)
Fe_2GeO_4	(γ) cubic	8·411	—	—	8	44·80	248·28	5·542	Durif-Varambon *et al.* (1956)
Co_2GeO_4	(γ) cubic	8·322	—	—	8	43·39	254·55	5·867	Durif-Varambon *et al.* (1956)
Ni_2GeO_4	(γ) cubic	8·221	—	—	8	41·83	254·01	6·072	Ringwood (1962)
Ni_2SiO_4	(γ) cubic	8·044	—	—	8	39·19	209·50	5·346	Yagi, Marumo & Akimoto (1974)
Fe_2SiO_4	(γ) cubic	8·234	—	—	8	42·03	203·78	4·848	Yagi *et al.* (1974)
Mn_2GeO_4	(β) orthorhombic	6·025	12·095	8·752	8	48·02	246·46	5·132	Morimoto *et al.* (1969)

Table 3

*Summary of isotropic elastic properties of polycrystalline germanates and silicates**

Compound	Structure	$\bar{M}$ (g)	V_m (cc/mole)	Density ($g\,cm^{-3}$)			Velocity ($km\,s^{-1}$)				Elastic moduli		Poisson's ratio
				X-ray	Bulk	% X-ray	v_p	v_s	v_ϕ	v_p/v_s	Bulk	Shear	
Mg_2GeO_4	Olivine (α)	26·46	45·87	4·038	3·97	98·3	7·40	4·22	5·57	1·75	1·25	0·72	0·259
$MgMnGeO_4$	Olivine (α)	30·83	48·96	4·408	4·35	98·7	6·65	3·62	5·17	1·84	1·18	0·58	0·289
Mn_2GeO_4	Olivine (α)	35·21	51·42	4·793	4·72	98·5	6·10	3·39	4·68	1·80	1·05	0·55	0·277
Ni_2SiO_4	Olivine (α)	29·93	42·51	4·928	4·80	97·4	7·29	4·15	5·49	1·76	1·49	0·85	0·260
Mg_2GeO_4	Spinel (γ)	26·46	42·35	4·373	4·32	98·6	8·54	4·90	6·40	1·74	1·79	1·05	0·255
Fe_2GeO_4	Spinel (γ)	35·47	44·80	5·542	5·46	98·6	7·14	3·63	5·78	1·97	1·85	0·73	0·326
Co_2GeO_4	Spinel (γ)	36·36	43·39	5·867	5·81	98·9	7·08	3·55	5·77	1·99	1·96	0·74	0·332
Ni_2GeO_4	Spinel (γ)	36·29	41·83	6·072	6·02	99·1	7·13	3·93	5·50	1·81	1·84	0·94	0·282
Ni_2SiO_4	Spinel (γ)	29·93	39·19	5·346	5·12	95·7	8·21	4·50	6·36	1·82	2·16	1·08	0·285
Fe_2SiO_4	Spinel (γ)	29·11	42·03	4·848	4·68	96·5	7·77	3·93	6·31	1·98	1·93	0·75	0·328
Mn_2GeO_4	Beta phase (β)	35·21	48·02	5·132	5·03	97·9	7·20	3·68	5·81	1·96	1·73	0·69	0·323

* All elastic property data are based on velocities at $P = 7{\cdot}5$ kbar and assuming the X-ray density for the compressed aggregate. Uncertainties are considered to be 0·1% for velocities or 0·2% for the elastic moduli. Data for α–$MgMnGeO_4$, γ–Ni_2SiO_4, and γ–Fe_2SiO_4 are presented here for the first time. Data for α–Mg_2GeO_4 and α–Mn_2GeO_4 are revised due to more precise pulse superposition measurements. All other data are unchanged from previous presentations (Liebermann 1972b, 1973a; Liebermann & Ringwood 1973).

Ni_2SiO_4; spinels—Mg_2GeO_4, Fe_2GeO_4, Co_2GeO_4, Ni_2GeO_4, Ni_2SiO_4, Fe_2SiO_4; beta phase—Mn_2GeO_4. A comprehensive description of the hot-pressing techniques employed in our laboratory is given elsewhere (Liebermann *et al.* 1975). The exact pressure and temperature conditions for the fabrication of the polycrystalline specimens (given in Table 1) were selected to be well inside the thermodynamic stability field of the relevant phase desired.

After sintering for 1–2 hr at elevated pressure and temperature, the hot-press run was cooled slowly (over 20–60 min) so as to retrieve polycrystalline aggregates which are not only single phase but also free of macroscopic cracks and suitable for ultrasonic measurements. The crystallographic structures of the specimens recovered at ambient conditions were confirmed by comparison of X-ray diffraction photographs with patterns from the literature (Table 2). Bulk densities determined by the Archimedes method and single-crystal X-ray densities are given in Tables 1 and 3, these specimens are less than 3 per cent porous (3·5 and 4·3 for γ–$Fe_2S_1O_4$ and γ–Ni_2SiO_4, respectively) and have a grain size always less than 100 μm and often less than 50 μm.

2.2 *Ultrasonic measurements*

The compressional (v_p) and shear (v_s) wave velocities in our recovered specimens were measured by the ultrasonic pulse superposition technique (McSkimin 1961) as modified for our small specimens (Liebermann 1973c; Liebermann *et al.* 1975). Lead zirconate–titanate transducers (PZT–5a, 5 MHz fundamental resonant frequency) were bonded to the ends of our cylindrical specimens with Dow Chemical resin 276–V9 and were used to transmit and receive the ultrasonic signals. With the transducers driven at their third or fifth harmonics (15–25 MHz carrier frequency), the precision of our velocity measurements is 0·02 per cent.

The pressure dependence of v_p and v_s in our specimens was determined as a function of hydrostatic pressure to 7·5 kbar. Specimens were jacketed from the fluid pressure medium (Dow-Corning, D.C-200 fluid, 1–3 centistoke viscosity) with the metal capsules in which they were fabricated. Temperature was monitored with a copper-constantan thermocouple and was maintained at 20 ± 1 °C.

As our specimens were hot-pressed in piston-cylinder or girdle apparati and we measure the velocities only along the cylindrical axis, there is a possibility that preferred orientation of grains produced by the triaxial hot-pressing could produce anomalous high or low values of velocity. We have attempted to minimize the likelihood of preferred orientation by surrounding the encapsulated specimen with polycrystalline rocksalt (NaCl) to provide a pseudohydrostatic pressure environment for the specimens fabricated at elevated pressures and temperatures. Moreover, we have shown previously that our polycrystalline specimens of α–Mg_2SiO_4 and the rutiles TiO_2 and GeO_2 are elastically isotropic within 1 per cent despite the extreme (> 25 per cent) velocity anisotropy of the single crystals of these minerals (Liebermann 1972b, 1973c). As the cubic spinel structure is even less likely to exhibit velocity anisotropy in polycrystalline aggregates, we assume that all of our specimens possess a comparable degree of elastic isotropy.

In addition to anisotropy, internal residual strain induced during hot-pressing may affect the elastic properties of polycrystalline materials (Spetzler 1970). While it is impossible to prove at this stage that such strains are not present in our specimens, we have attempted to minimize these effects by using NaCl as a pressure medium and by annealing the specimens during the cooling and decompression cycle of our hot-pressing runs.

3. Elasticity data

The velocity *vs* pressure data (corrected for length change upon compression) for our germanate and silicate polycrystalline specimens are illustrated in Figs 1–11;

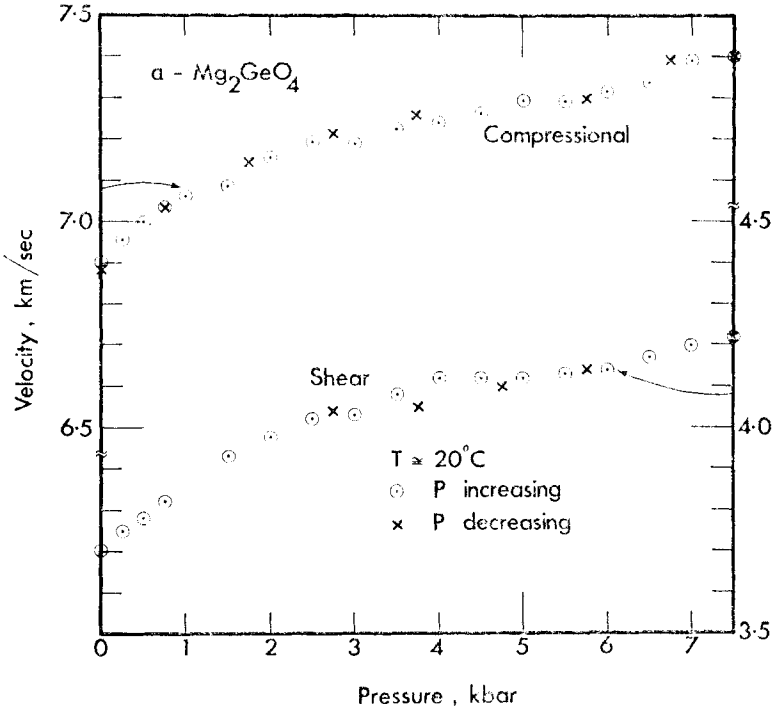

FIG. 1.

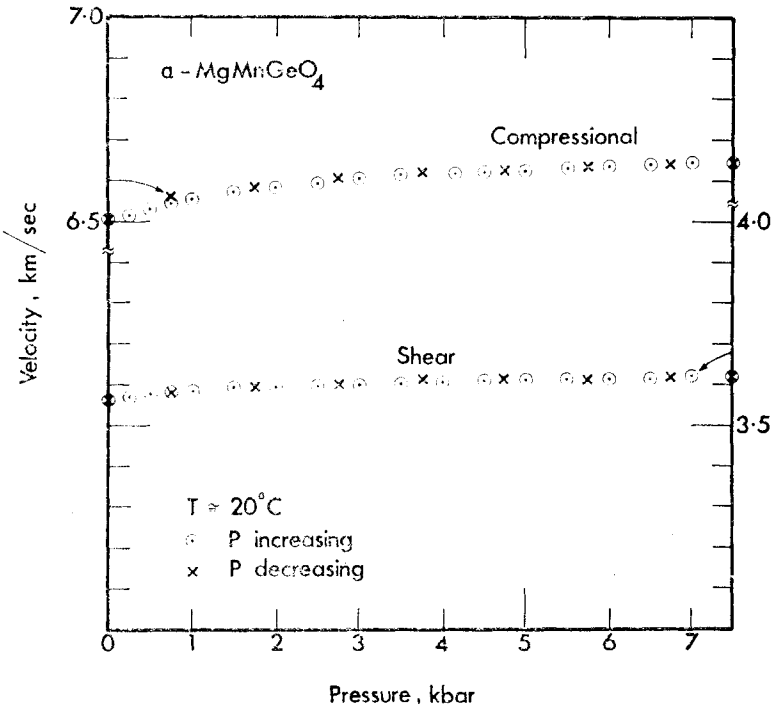

FIG. 2.

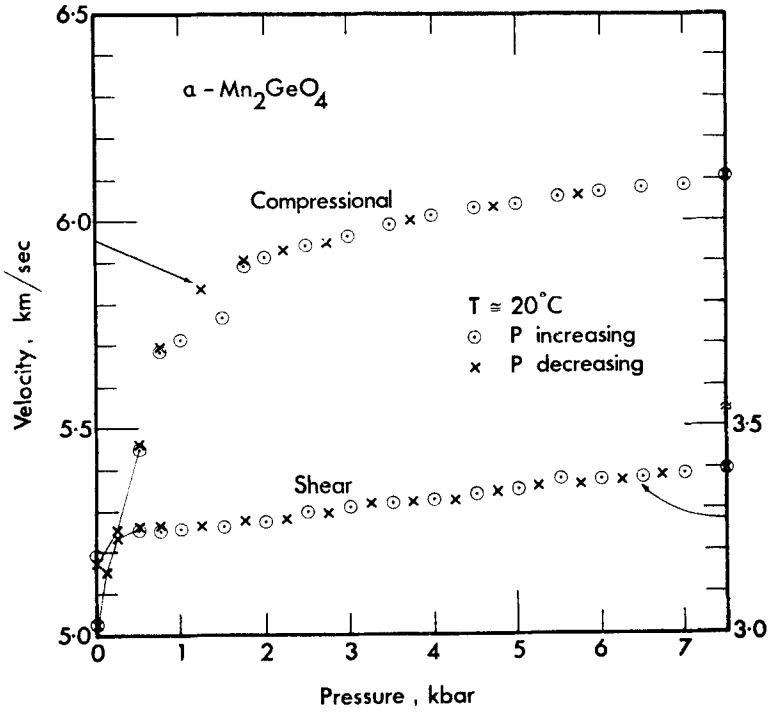

FIG. 3.

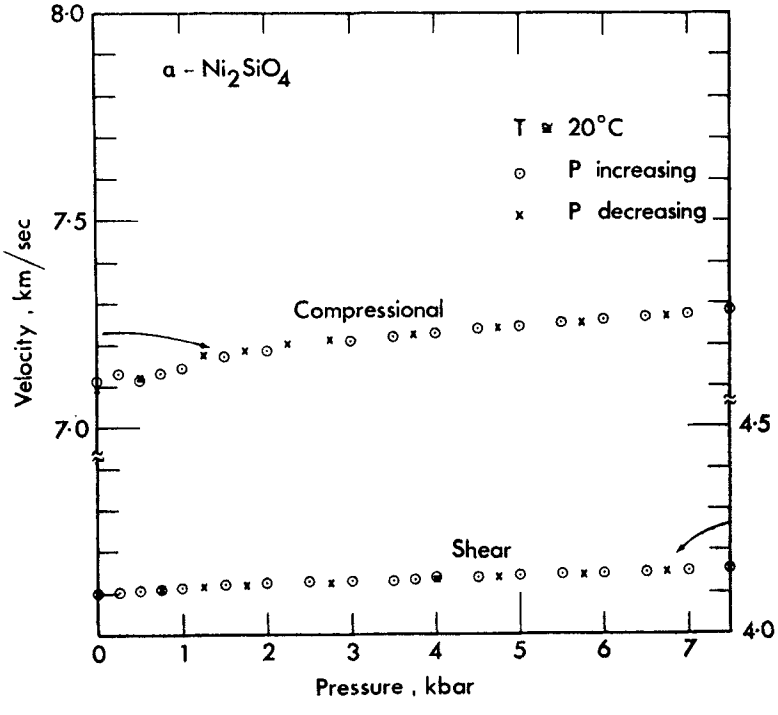

FIG. 4.

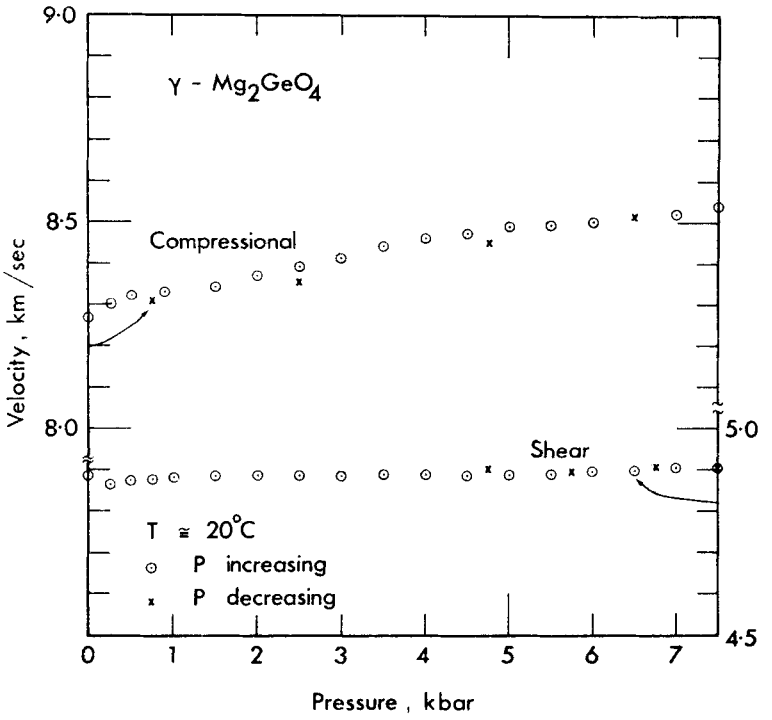

FIG. 5.

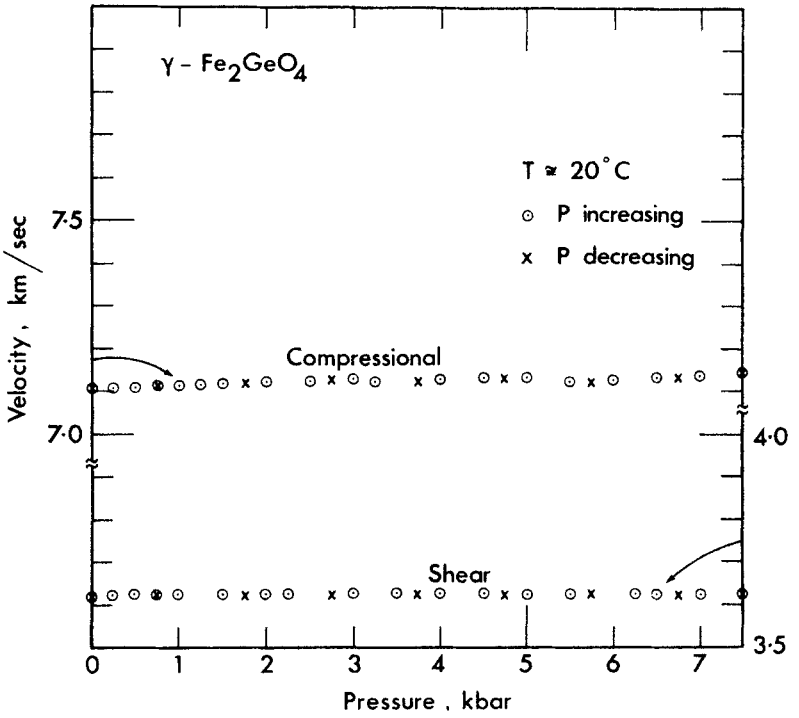

FIG. 6.

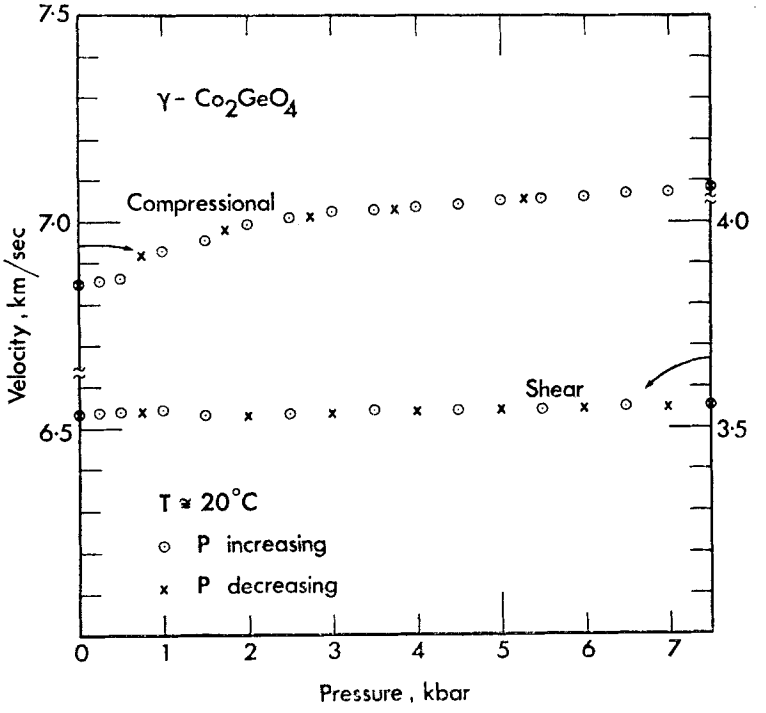

FIG. 7.

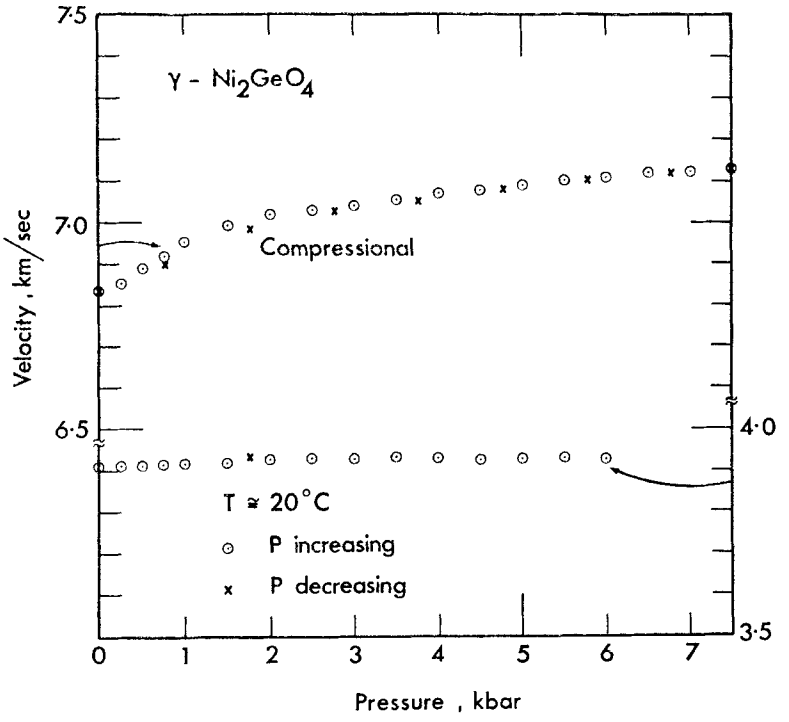

FIG. 8.

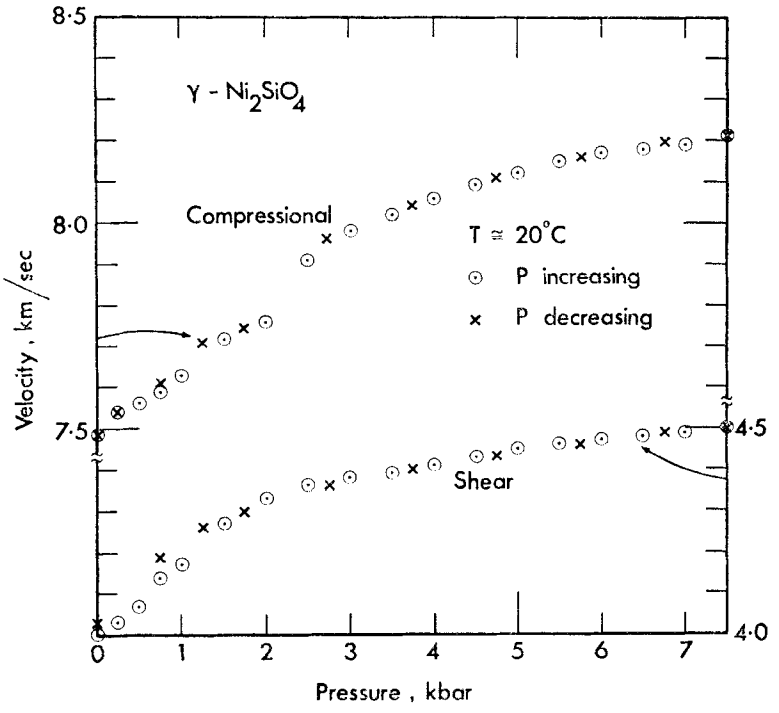

FIG. 9.

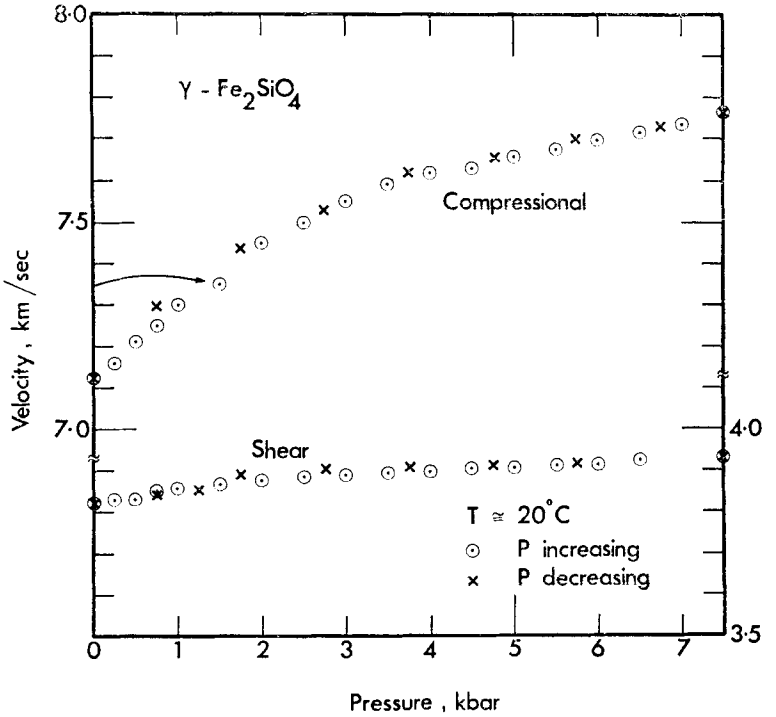

FIG. 10.

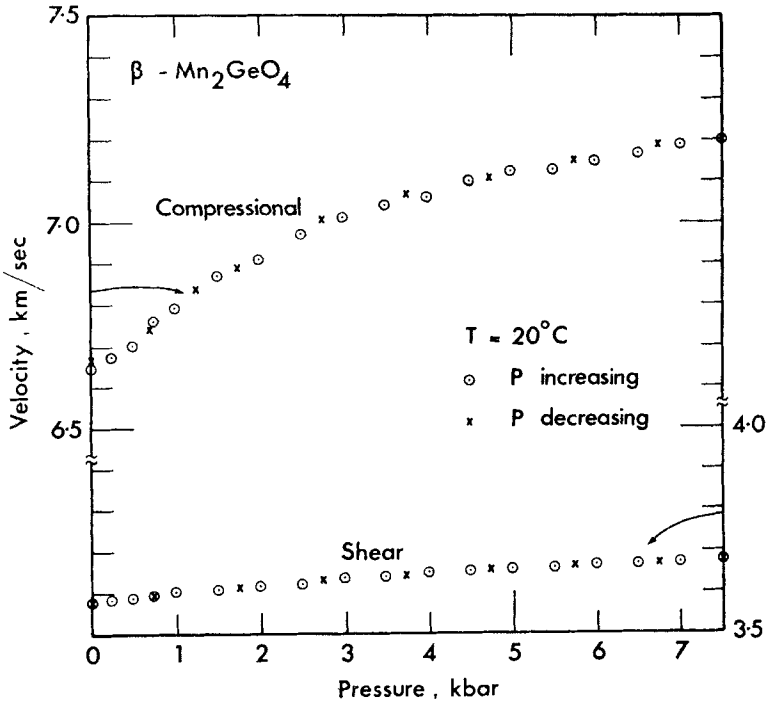

FIGS 1–11. Compressional and shear velocities *vs* pressure at room temperature for polycrystalline specimens of various phases listed in Tables 1 and 3 using the ultrasonic pulse superposition technique. Precision of individual velocity determinations is 0·02 per cent.

both v_p and v_s increase monotonically with increasing pressure and these changes are completely reversible on release of pressure. In general, the velocities increase rather rapidly in the range $P = 0$–3 kbar and then are constant or only increase slightly with higher pressures. For several specimens (e.g. Figs 1, 5, 9–11) the compressional velocity appears to be increasing steadily at the highest pressures; however, subsequent experiments have demonstrated that for these specimens the compressional velocity achieves a stable plateau value for $P = 6$–10 kbar. We interpret these initial velocity increases to be the result of closing microcracks and eliminating residual porosity. In some of our specimens, the observed increases in velocity are somewhat larger than would be expected (Mackenzie 1950) from the bulk densities if the pores were spherical (e.g. v_p and v_s for α–Mg_2GeO_4, α–Mn_2GeO_4, and v_p for γ–Ni_2GeO_4, β–Mn_2GeO_4). Our specimen of Fe_2GeO_4 spinel is a particularly good polycrystalline aggregate for ultrasonic measurements. In Fig. 12, we illustrate the observed echo pattern for shear waves of 15 MHz carrier frequency. The precision of the velocity determinations for this specimen is 1×10^{-4}. Both v_p and v_s increase linearly over the pressure range $P = 0$–7·5 kbar (Fig. 6); the observed increases are comparable to those measured for single crystals of magnesium–iron aluminate spinels (Schreiber 1967; Wang & Simmons 1972; Chang & Barsch 1973). We are currently refining these data and will report subsequently the pressure derivatives of the velocities for this important germanate spinel.

We take the velocity data at $P = 7{\cdot}5$ kbar to be representative of those of the zero-porosity, elastically-isotropic polycrystalline aggregate. On this basis, we adopt the X-ray density and calculate the adiabatic elastic moduli and Poisson's ratio from the equations for an isotropic elastic medium. These data are summarized in Table 3.

While the inherent precision of the pulse superposition data in Figs 1–11 is 0·02 per cent, other experimental uncertainties imply a precision of 0·1 per cent for the velocities given in Table 3 (or 0·2 per cent for the elastic moduli).

Of the 11 phases investigated in the present study, four have been the subject of ultrasonic work in other laboratories. Soga (1971) measured v_p and v_s for two porous (4·4 and 1·9 per cent) polycrystalline aggregates of α–Mg_2GeO_4 and extrapolated these data to estimate $v_p = 7{\cdot}4 \pm 0{\cdot}1$ km s^{-1} and $v_s = 4{\cdot}4 \pm 0{\cdot}2$ km s^{-1} for a zero-porosity specimen (see Table 7). Our values of $v_p = 7{\cdot}40$ km s^{-1} and $v_s = 4{\cdot}22$ km s^{-1} agree with Soga's within the dual uncertainties. Mizutani *et al.* (1970; see also Akimoto 1972) determined v_p and v_s at confining pressures of $P = 6$ kbar for a polycrystalline specimen of γ–Fe_2SiO_4 recovered after hot-pressing at $P = 75$ kbar and $T = 900$ °C; their values ($v_p = 8{\cdot}05$, $v_s = 4{\cdot}10$) are somewhat higher than ours ($v_p = 7{\cdot}77$, $v_s = 3{\cdot}93$). The sources of this discrepancy are not known at present, but may be related to fact that v_p for our specimen is still increasing systematically at $P = 7{\cdot}5$ kbar (Fig. 10). Interlaboratory comparisons are underway to resolve the uncertainty in the data for this and other materials (H. Mizutani, private communication, January 1974). Chung (1973, 1974) has estimated the elastic properties of α–Mg_2GeO_4, γ–Mg_2GeO_4 and γ–Fe_2GeO_4 from measurements on composite polycrystals of the sample powder embedded in a matrix of AgCl; his data* are in accord with the data of our laboratory (Liebermann 1972b, 1973a; Liebermann & Ringwood 1973).

We may also compare our ultrasonically-determined values of K_0 (the zero-pressure bulk modulus) with determinations of this quantity from static compression data for γ-Fe_2SiO_4 and γ–Ni_2SiO_4 (Mao *et al.* 1969; Mao, Takahashi & Bassett 1970). The ultrasonic data are 10–13 per cent lower than the static values which were derived by fitting a Birch–Murnaghan equation with $K_0' = (\partial K_s/\partial P)_{T;\,P=0} \equiv 4$ to the assemblage of P–V data. The static determinations of K_0 are very sensitive to the value adopted for K_0' (e.g. Bassett & Barnett 1970; Liu, Bassett & Takahashi 1974) and some of the discrepancy with the ultrasonic data may be due to this uncertainty. However, it would require $K_0' \equiv 6$ for γ–Fe_2SiO_4 and $K_0' \equiv 7$ for γ–Ni_2SiO_4 for the static data to completely remove the discrepancy (Liu, private communication) and these values of K_0' are unreasonably large for spinel compounds.

	K_0 Mbar	
	Ultrasonic	Static
γ–Fe_2SiO_4	1·93	2·12
γ–Ni_2SiO_4	1·87	2·14

4. Discussion

The major goal of our experimental program is to determine the elastic properties of the low-pressure and high-pressure polymorphs for a wide variety of crystallographic phase transformations thought to be relevant to discussions of the Earth's interior. It is important to attempt to discern characteristics which relate the

* Chung (1974) has also presented data for Fe_2GeO_4 olivine, data to which we have referred to previously (Liebermann & Ringwood 1973; Liebermann 1973b). Since then we have tried unsuccessfully to synthesize this olivine phase at atmospheric pressure and temperatures ranging up to the melting point ($T \approx 1200$ °C); in all cases, the quench product was the spinel form. Furthermore, an extensive literature research has revealed no indication of the existence of Fe_2GeO_4, Co_2GeO_4 or Ni_2GeO_4 in the olivine form (Durif-Varambon, Bertaut & Pauthenet 1956, Table 1; Ringwood 1958, p. 22; Dachille & Roy 1960; Mathur, Sinha & Yagnik 1965; Navrotsky & Kleppa 1968, pp. 497–498; Kamb 1968, p. 1448; Hariya & Wai 1970, p. 360; Navrotsky 1973). Consequently, the Fe_2GeO_4 olivine data of Chung (1974) must be viewed with reserve until adequate experimental details are provided.

elasticity and crystallographic data for these polymorphs because, if such relationships do exist, they could provide the basis for predicting the elasticity of phases whose properties cannot or have not yet been measured. These relationships could also be employed as constraints in attempts to construct or interpret geophysical models for the elastic properties of the transition zone in the Earth's mantle (e.g. Liebermann 1973b).

4.1 *Velocity–density systematics across phase transformations*

Our new elasticity data for the olivine–spinel and olivine–beta phase transformations are combined in Table 4 with the crystallographic data of previous investigators to compare the density and velocity jumps across these polymorphic transitions (see also brief discussion in Liebermann 1973b). For the olivine–spinel transitions, the zero-pressure density jumps are 8–10 per cent, whereas the velocity jumps are 12–20 per cent, or roughly $1\frac{1}{2}$–2 times the density change (except v_s for Ni_2SiO_4). This relationship of density and velocity jumps has been previously noted for v_p (Mizutani *et al.* 1970; Liebermann 1972b). Note especially that for a given compound the changes of v_p, v_s and v_ϕ (bulk sound velocity) are comparable in percentage magnitude. For the olivine–beta transition in Mn_2GeO_4, the jumps in v_p and v_ϕ are roughly three times as large as the density jump, while the shear velocity change is of comparable percentage magnitude to the density change. In a later section of this paper, we shall compare these experimental data with velocity and density discontinuities near 400-km depth in recent Earth models.

Also listed in Table 4 are the v_p/v_s ratios for the low-pressure and high-pressure polymorphs of various compounds. This ratio is approximately constant or increases slightly for the olivine–spinel transformation, while for the one example of the olivine–beta phase transformation the ratio increases markedly as a consequence of the relatively small jump in shear velocity. Similar results have been found for the pyroxene-garnet and pyroxene-ilmenite transitions (Liebermann 1974) and this tendency for v_p/v_s (and thus Poisson's ratio) to increase across crystallographic phase transformations at constant chemical composition may prove to be a very powerful constraint in constructing or testing Earth models in the vicinity of the transition zone.

Many empirical laws describing velocity–density systematics have been proposed by previous investigators; most of these imply a unique dependence of elastic wave velocity v upon density ρ for materials of common mean atomic weight $\overline{M}$, irrespective of whether the density changes are due to variations of crystallographic structure, pressure, or temperature. In an earlier paper, we have demonstrated that v–ρ relationships across such transitions are not always equivalent to v–ρ changes caused by compression or thermal expansion of a homogeneous material, or by variations of composition at constant $\overline{M}$ (Liebermann & Ringwood 1973). In Table 5, we present a more complete evaluation of the applicability of such empirical laws to the olivine–spinel (α–γ) and olivine–beta phase (α–β) data of this paper.

Table 4

Density and velocity jumps across polymorphic phase transformations

Phase transformation	Compound	$\Delta\rho$	Δv_p	Δv_s	Δv_ϕ	v_p/v_s
			%			LP–HP
Olivine-spinel	Mg_2GeO_4	8	15	16	15	1·75–1·74
Olivine-spinel	Ni_2SiO_4	8	13	8	16	1·76–1·82
Olivine-spinel	Fe_2SiO_4	10	17	13	20	1·90–1·98
Olivine-beta phase	Mn_2GeO_4	7	18	9	24	1·80–1·96

FIG. 12. Pulse superposition echo pattern for shear waves in Fe_2GeO_4-spinel at $P = 1$ bar, $T = 20\,^{\circ}C$. Carrier frequency is 15 MHz and pulse repetition frequency is $487{\cdot}6 \pm 0{\cdot}1$ kHz.

facing page 912

A brief summary of the more common velocity–density systematic relationships is appropriate. Birch (1961a, b) demonstrated a linear relationship between compressional velocity v_p and density ρ for rocks and minerals of common mean atomic weight $\bar{M}$:

$$v_p = a(\bar{M}) + b\rho \tag{1}$$

with $a = -1{\cdot}87$ and $b = 3{\cdot}05$ for $\bar{M} = 20$–22. This parameterization of the linear v_p–ρ curves on the basis of a $(\bar{M})$ (with b assumed independent of $\bar{M}$) has become known as ' Birch's law ' and plots of velocity versus density as ' Birch diagrams '. For the bulk sound velocity $v_\phi = (K_s/\rho)^{\frac{1}{2}}$ where K_s is the adiabatic bulk modulus, Wang (1968a, b, 1969, 1970) has shown that:

$$v_\phi = A(\bar{M}) + B\rho \tag{2}$$

with $A(\bar{M}) = -1{\cdot}75$, $B = 2{\cdot}36$ for Wang's preferred solution for $\bar{M} = 20{\cdot}2$–$22{\cdot}2$ (Wang 1968b, 1972).

Birch also speculated that, for a given substance, equation (1) would describe changes of v_p and ρ produced by isothermal compression, isobaric expansion or polymorphic phase transformations. Ultrasonic data for the pressure and tempera-

Table 5

Comparison of parameters for velocity–density relationships for density changes produced by phase transformations, isothermal compression, isobaric expansion or variation of composition of constant mean atomic weight.

		b	λ_p	B	λ_ϕ	n	X
Phase transformations[1]	α–γ Mg_2GeO_4	3·4	1·8	2·5	1·7	0·29	4·5
	α–γ Fe_2SiO_4	2·5	1·6	2·3	1·8	0·27	4·7
	α–γ Ni_2SiO_4	2·2	1·4	2·1	1·8	0·28	4·6
	α–β Mn_2GeO_4	3·2	2·4	3·3	3·2	0·16	7·3
Thermodynamic	Compression	3·2[2]	1·3[3]	3·5[2]	2·0[3]	0·25[4]	5·0[4]
	Expansion	5·3[2]	2·0[3]	3·3[2]	1·9[3]	0·26[4]	4·8[4]
Empirical	$\bar{M} = 20$–21	3·1[5]	1·25[6]	2·4[7]	1·25[6]	0·33[8]	4·0[9]

Notation:	Phase transformation	Compression	Expansion
b	$\Delta v_p/\Delta\rho$	$(K_T/\rho)(\partial v_p/\partial P)_T$	$-(\alpha_v\rho)^{-1}(\partial v_p/\partial T)_p$
λ_p	$(\partial \ln v_p/\partial \ln \rho)$	$(K_T/v_p)(\partial v_p/\partial P)_T$	$-(\alpha_v v_p)^{-1}(\partial v_p/\partial T)_p$
B	$\Delta v_\phi/\Delta\rho$	$(v_\phi/2\rho)(K_0'-1)$	$(v_\phi/2\rho)(\delta_s-1)$
λ_ϕ	$(\partial \ln v_\phi/\partial \ln \rho)$	$1/2(K_0'-1)$	$1/2(\delta_s-1)$
n	$(\partial \ln(\rho/\bar{M})/\partial \ln \phi)$	$(K_0'-1)^{-1}$	$(\delta_s-1)^{-1}$
X	$-(\partial \ln K_s/\partial \ln V)$	K_0'	δ_s

where:

K_T isothermal bulk modulus; α_v volume thermal expansion;

$K_0' = (\partial K_s/\partial P)_{T;\,P=0}$, $\quad \delta_s = -(\alpha_v K_s)^{-1}(\partial K_s/\partial T)_p$

[1] Changes in these parameters from those given by Liebermann & Ringwood (1973) are primarily the result of the more precise velocity data presented here for Mg_2GeO_4 and Mn_2GeO_4 phases and our new velocity data for γ-Fe_2SiO_4 and γ-Ni_2SiO_4.

[2] Liebermann & Ringwood (1973); Wang (1970); Anderson, D. L. *et al.* (1971).

[3] Anderson, O. L. (1973); Wang (1970).

[4] Follow directly from λ_ϕ via $n = (2\lambda_\phi)^{-1}$ and $X = 2\lambda_\phi + 1$.

[5] Birch (1961a).

[6] Shankland & Chung (1974).

[7] Wang (1968a, b, 1972).

[8] Anderson, D. L. & Kanamori (1968).

[9] Anderson, O. L. & Nafe (1965).

ture derivatives of the velocities enable us to calculate the v–ρ trajectories due to isothermal compression: $(\partial v_i/\partial\rho)_T = (K_T/\rho)(\partial v_i/\partial P)_T$ or isobaric expansion: $(\partial v_i/\partial\rho)_P = -(\alpha_V\,\rho)^{-1}(\partial v_i/\partial T)_P$ where K_T = isothermal bulk modulus and α_V = volume thermal expansion. These thermodynamic values of b^T and B^T have been calculated by a number of authors (e.g. Wang 1970; Anderson, D. L., Sammis & Jordan 1971) and representative values are given in Table 5 for compounds with $\overline{M} = 20$–21.

For the α–γ and α–β phase transformations, we calculate $b^P = \Delta v_p/\Delta\rho$ and $B^P = \Delta v_\phi/\Delta\rho$ directly from the density and velocity jumps across the transitions and compare these values in Table 5 with those derived from thermodynamic data (b^T and B^T) and from the empirical correlations (b and B) of equations (1) and (2). For compressional velocity, we note that $b^T \cong b^P \cong b$, thus supporting Birch's conjecture. In contrast, for the bulk sound velocity, $B^T < B^P \cong B$ for the α–γ transition while $B^T \cong B^P > B$ for the α–β transition. The discrepancy between B^T and B values is most likely due to the particular data set chosen by Wang (1968a, b, 1972) to fit equation (2) for $\overline{M} = 20$–22. For the α–γ transition, there is a definite tendency for both b^P and B^P to decrease with increasing $\overline{M}$. Similar behaviour has been observed for the quartz–rutile (Soga 1971) and pyroxene–garnet and pyroxene–ilmenite (Liebermann 1974) transformations and casts doubt, on the validity of attempts to predict the elastic properties of high-pressure phases using the linear form of Birch's law with constant b or B values.

Several investigators have shown that Birch's law may be considered as a linearization, over a limited range of density, of a power law relating velocity to density:

$$v_i = C(\overline{M})\,\rho^{\lambda i}. \tag{3}$$

This relationship for the bulk sound velocity v_ϕ follows directly from the law of corresponding states: $K_s = AV_0^{-x}$ (Anderson, O. L. & Nafe 1965); the seismic equation of state: $\rho/\overline{M} = A(\overline{M})\,\phi^n$ where $\phi = K_s/\rho$ is the seismic parameter (Anderson, D. L. 1967); and the power law formulations of Birch's law (Shankland 1972; Chung 1972). Since all of these semi-empirical laws are really equivalent representations of the relationship of bulk modulus to volume for materials of common $\overline{M}$ (Anderson, O. L. 1973), a discussion of λ_ϕ will suffice for all. For the seismic equation of state ($n = \frac{1}{3}$) and the law of corresponding states ($x = 4$)$\lambda_\phi \cong 1{\cdot}5$ from empirical observations. Shankland & Chung (1974) have found that $\lambda_\phi = 1{\cdot}25$ for $\overline{M} \cong 20{\cdot}2$ and $\lambda_\phi \cong 1{\cdot}7$ for the more limited data for $\overline{M} = 35$.

Thermodynamic values of λ_ϕ can again be calculated from the pressure and temperature derivatives of the bulk modulus. For isothermal compression, $\lambda_\phi = \frac{1}{2}(K_0' - 1)$ where $K_0' = (\partial K_s/\partial P)_{T/\,P=0}$ and for isobaric expansion, $\lambda_\phi = \frac{1}{2}(\delta_s - 1)$ where $\delta_s = -(\alpha_V\,K_s)^{-1}(\partial K_s/\partial T)_P$. These thermodynamic ($\lambda_\phi{}^T$) values are compared in Table 5 with those derived from the α–γ and α–β phase transition data $\lambda_\phi{}^P = (\partial \ln v_\phi/\partial \ln\rho)$ and the empirical correlations (λ_ϕ) above. We observe that $\lambda_\phi{}^P \cong \lambda_\phi{}^T > \lambda_\phi$ for the α–γ transition and $\lambda_\phi{}^P > \lambda_\phi{}^T > \lambda_\phi$ for the α–β transition. Note that $\lambda_\phi{}^P$ is virtually independent of $\overline{M}$ for the olivine–spinel transformation, a tendency which has also been observed for the quartz–rutile, pyroxene–garnet, and pyroxene–ilmenite transitions (Liebermann & Ringwood 1973; Liebermann 1974). Thus, we cannot seek an explanation for the high value of λ_ϕ for the α–β transition in Mn_2GeO_4 in terms of its large mean atomic weight ($\overline{M} = 35{\cdot}2$) as might have been suggested by the dependence of λ_ϕ upon $\overline{M}$ observed by Shankland & Chung (1974).

We conclude from the power-law discussion that the changes in velocity and density produced by the olivine–spinel phase transformation in germanate and silicate compounds are consistent with those derived from thermodynamic data for isothermal compression or isobaric expansion of a homogeneous material; the changes produced by the olivine–beta phase transformation in Mn_2GeO_4 are somewhat greater than those predicted from the thermodynamic data.

Table 6

Co-ordination and nearest-neighbour distances in A_2BO_4 and SiO_2 polymorphs

Compound	Structure	Co-ordination	Nearest-neighbour distance Å	
			A–O	B–O
Mg_2SiO_4	olivine[1]	6–4–4	2·119	1·634
	beta[2]	6–4–(5, 4, 3)	2·09	1·64
Co_2SiO_4	olivine[3]	6–4–4	2·134	1·627
	beta[3]	6–4–(5, 4, 3)	2·114	1·642
	spinel[3]	6-4–4	2·104	1·646
Fe_2SiO_4	olivine[4]	6–4–4	2·169	1·638
	spinel[5]	6–4–4	2·137	1·652
Ni_2SiO_4	olivine	6–4–4	—	—
	spinel[5]	6-4–4	2·063	1·654
Mn_2GeO_4	olivine	6–4–4	(2·21)[10]	(1·75)[10]
	beta[6]	6–4–(5, 4, 3)	2·189	1·770
	delta[6]	7–6–5	2·283	1·971
SiO_2	α-quartz[7]	4–2	1·607	—
	coesite[8]	4–2	1·613	—
	rutile[9]	6–3	1·783	—

[1] Birle *et al.* (1969); actual composition $(Mg_{0.9}Fe_{0.1})_2SiO_4$.

[2] Moore & Smith (1970); actual composition $(Mg_{0.9}Ni_{0.1})_2SiO_4$.

[3] Morimoto *et al.* (1974); in the spinel polymorph, 3·4±0·8 per cent of the Si atoms are in 6-fold co-ordination.

[4] Birle *et al.* (1969); actual composition $(Mg_{0.04}Fe_{0.92}Mn_{0.04})_2SiO_4$.

[5] Yagi *et al.* (1974); in the spinel polymorphs of Fe_2SiO_4 and Ni_2SiO_4, 2·3±1·0 per cent and 0·5±1·2 per cent, respectively, of the Si atoms are in 6-fold co-ordination.

[6] Morimoto, Tokonami & Koto (1972); delta = strontium plumbate structure.

[7] Smith & Alexander (1963).

[8] Zoltai & Buerger (1959).

[9] Liu (1970).

[10] Mn–O and Ge–O distances are estimated from those exhibited by the orthoenstatite $MnGeO_3$ (Fang, Townes & Robonson 1969) which has 6–4–(4, 3) co-ordination (Shannon & Prewitt 1969). Compare also with distances of 2·22 Å in MnO (rocksalt) and 1·739 in α–GeO_2 (Smith & Isaacs 1964).

Anderson, O. L. (1973) has pointed out that values of $\lambda_\phi{}^P$ computed from measured data across phase transformations will depend critically on the equation of state employed. We have used $\lambda_\phi{}^P$ = const, which is equivalent to the Murnaghan equation of state (Anderson, D. L. 1967) in which $K' = (\partial K_s/\partial P)_T$ is independent of pressure (or density). For phase transitions characterized by large density increases (e.g. 47 per cent for coesite–rutile in SiO_2 and 36 per cent for feldspar–hollandite in $NaAlGe_3O_8$) we should anticipate that our $\lambda_\phi{}^P$ will be lower than the thermodynamically determined values of $\lambda_\phi{}^T$ for isothermal compression of the low-pressure phase. However, for the α–γ and α–β transitions discussed here, the density increases are only 7–10 per cent so that the computed values of $\lambda_\phi{}^P$ are not sensitive to the particular equation of state adopted.

The relatively high slopes (linear or logarithmic) on v–ρ diagrams determined here for the olivine–spinel and olivine–beta phase transformations are similar to the behaviour observed for the quartz–coesite transition in SiO_2. These transitions involve no change in co-ordination of Ge or Si with respect to oxyxen and no change in cation–anion distances (Table 6). By contrast, the coesite–rutile, pyroxene–garnet

Table 7

Summary of isotropic elastic properties of other olivine and spinel compounds from ultrasonic studies.

Compound	Structure	$\tilde{M}$	V	Density	Velocity				Elastic moduli		Poisson's ratio	Reference
		(g)	(cc/mole)	(g cm^{-3})	(km s^{-1})				(Mbar)			
					v_p	v_s	v_ϕ	v_p/v_s	Ks	μ	σ	
Mg_2SiO_4	Olivine	20·12	43·68	3·224	8·57	5·02	6·32	1·71	1·286	0·811	0·240	1
Mg_2SiO_4	Olivine	20·10	43·67	3·222	8·59	5·03	6·33	1·71	1·291	0·816	0·239	2
$(Mg_{0.93}Fe_{0.07})SiO_4$	Olivine	20·79	43·95	3·311	8·42	4·89	6·25	1·72	1·29	0·791	0·246	1
Fe_2SiO_4	Olivine	29·10	46·39	4·393	6·64	3·49	5·27	1·90	1·220	0·536	0·308	3
Mg_2GeO_4	Olivine	26·46	45·87	4·038	7·4	4·4	5·4	1·7	1·2	0·78	0·23	4
$MgAl_2O_4$	Spinel	20·32	39·76	3·578	9·78	5·50	7·43	1·78	1·974	1·084	0·268	5
$Mg_{0.75}Fe_{0.36}Al_{1.9}O_4$	Spinel	21·8	40·35	3·826	9·27	5·04	7·21	1·84	1·992	0·972	0·290	6
$FeAl_2O_4$	Spinel	24·8	40·61	4·280	8·70	4·46	7·01	1·95	2·104	0·851	0·322	6
$MnFe_2O_4$	Spinel	32·95	45·62	5·051	7·42	3·71	6·05	2·00	1·85	0·69	0·332	7, 8
$NiFe_2O_4$	Spinel	33·49	44·12	5·313	7·23	3·66	5·86	1·98	1·82	0·713	0·327	7, 8
$FeFe_2O_4$	Spinel	33·08	44·85	5·163	7·19	4·27	5·23	1·68	1·41	0·94	0·228	9
Fe_2SiO_4	Spinel	29·10	42·03	4·848	8·05	4·10	6·51	1·96	2·05	0·81	0·316	10, 11

[1] Kumazawa & Anderson, O. L. (1969)
[2] Graham & Barsch (1969)
[3] Chung (1970)
[4] Soga (1971)
[5] Chang & Barsch (1973)
[6] Wang & Simmons (1972)
[7] Liebermann (1970)
[8] Liebermann (1972c)
[9] Simmons & England (1969)
[10] Mizutani *et al.* (1970)
[11] Akimoto (1972)

Table 8

Parameters of law of corresponding states and Shankland-Chung relationship for isomorphic series.

Structure	Compound	$K_0 V_0$ (Mbar)·(cc/mole)	$V\phi\bar{M}^{\frac{1}{2}}$ (km s^{-1})·(g)$^{\frac{1}{2}}$
Olivine	Mg_2GeO_4	57·3	28·7
	$MgMnGeO_4$	57·8	28·7
	Mn_2GeO_4	54·0	27·8
	Ni_2SiO_4	63·3	30·0
	Fe_2SiO_4	56·6	28·4
	Mg_2SiO_4	56·3	28·4
	$(Mg_{0.93}Fe_{0.07})_2SiO_4$	56·7	28·5
Spinel	Mg_2GeO_4	75·8	32·9
	Fe_2GeO_4	82·9	34·4
	Co_2GeO_4	85·0	34·8
	Ni_2GeO_4	77·0	33·1
	Ni_2SiO_4	84·7	34·8
	Fe_2SiO_4	81·1–86·2	34·0–35·1
	$MgAl_2O_4$	78·5	33·5
	$Mg_{0.75}Fe_{0.36}Al_{1.9}O_4$	80·4	33·7
	$FeAl_2O_4$	85·4	34·9
	$MnFe_2O_4$	84·4	34·7
	$NiFe_2O_4$	80·3	33·9
Beta	Mn_2GeO_4	83·1	34·5

and pyroxene–ilmenite transitions are characterized by low v–ρ slopes and involve major increases in cation co-ordination and cation–anion distance (Liebermann 1974). This dependence of the v–ρ slopes on co-ordination has also been noted by Davies (1974) for transitions which involve isochemical mixed oxides as the transformation product. That such trends may not be universal is demonstrated by the fact that the quartz–rutile transition in GeO_2 exhibits values of $\lambda_p = 1{\cdot}9$ and $\lambda_\phi = 2{\cdot}1$, and yet involves a change of cation co-ordination from 4-fold to 6-fold.

Shaw's (1974) data for the elastic properties across the rocksalt to caesium chloride phase transition in Rb halides also exhibit low logarithmic v–ρ slopes. For these transformations, in which the cation–anion co-ordination increases from 6-fold to 8-fold while the interatomic distances also increase, $\lambda_\phi{}^P \cong 0{\cdot}1$ which is very much less than $\lambda_\phi{}^T \cong 2{\cdot}2$ for isothermal compression of the low-pressure rocksalt phase.

Co-ordination changes and nearest-neighbour cation–anion distances thus appear to be important factors in determining elasticity variations across polymorphic phase transitions in crystalline solids. These qualitative observations are developed further and placed on a more quantitative basis in a subsequent paper (Liebermann & Ringwood 1974b). The distinction between phase transformations which involve constant or increased cation co-ordinations may also be an important diagnostic tool for interpreting geophysical models of the Earth's interior in terms of composition and mineralogy (Liebermann & Ringwood 1974a).

4.2 *Velocity–density systematics in isomorphic series*

In recent years, there has been considerable effort in solid-state geophysics to establish patterns relating the elastic properties to other physical properties such as

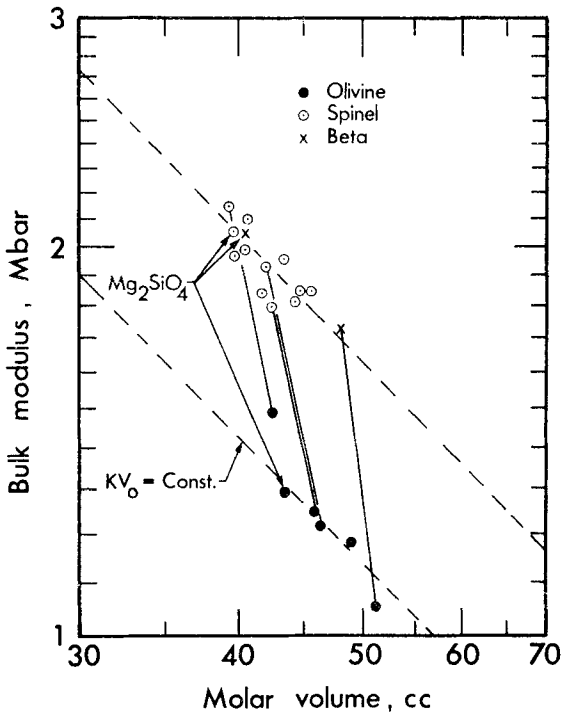

FIG. 13. Log–log plot of bulk modulus K_s *vs* volume V_0 for compounds with olivine, spinel and beta phase structures. $K_s V_0$ = const. lines represent isostructural series (following O. L. Anderson & Nafe 1965; and D. L. Anderson & O. L. Anderson 1970).

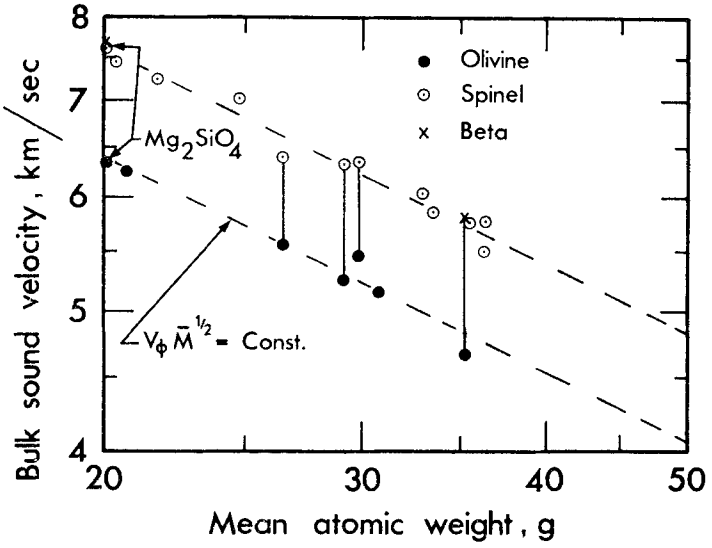

FIG. 14. Log–log plot of bulk sound velocity v_ϕ *vs* mean atomic weight $\bar{M}$ for compounds with olivine, spinel and beta phase structures. The $v_\phi \bar{M}^{\frac{1}{2}}$ = const. lines represent isostructural series (following Shankland 1972; Chung 1972).

Table 9

Elasticity of Mg_2SiO_4 in olivine and spinel phases.

Structure	$\bar{M}$ (g)	V_0 cc/mole	ρ_0 (g cm^{-3})	$K_0 V_0$	K_0 Mbar	v_ϕ (km s^{-1})	$v_\phi \bar{M}^{\frac{1}{2}}$	v_ϕ (km s^{-1})
Olivine	20·10	43·79[1]	3·21	56·3	1·29	6·32	28·4	6·32
Spinel	20·10	39·58[2]	3·56	81·6[3]	(2·06±0·05)	(7·6±0·1)	34·1	(7·6±0·1)

[1] Robie *et al.* (1966).

[2] Ringwood & Major (1970) based on extrapolated lattice parameter.

[3] Underlined values assumed, following trends in Table 8.

[4] Values in parentheses are predicted on basis of systematic trends in Table 8.

molar volume, density, and mean atomic weight for compounds belonging to the same crystal class. In this section, we show how the olivine, spinel and beta phase data for our germanate and silicate compounds fit several of these semi-empirical patterns and demonstrate the usefulness of such trends by predictions of the elasticity of Mg_2SiO_4 in the spinel and beta phase structures.

Several previous investigations have shown that the bulk modulus K_s is inversely proportional to the volume for isostructural sequences of alkali halides, fluorides, oxides and other chalcogenides (e.g. Anderson, O. L. & Nafe, J. E. 1965; Anderson, D. L. & Anderson, O. L., 1970). In Fig. 13 we plot our new germanate and silicate data and other available data for the olivine and spinel structures (Table 7) in a diagram of $\log K_s$ against $\log V_0$, where V_0 is the molar volume. For the olivine structure, the relationship $K_s V_0 = \text{const}$ holds very well as is demonstrated in Table 8, with the notable exception of α–Ni_2SiO_4. Previously, data for the relatively open-packed olivine structure did not appear to be consistent with the $K_s V_0 = \text{const}$ law (Anderson, D. L. & Anderson, O. L. 1970), but it was difficult to test this conclusion because of the small variation (6 per cent) in molar volumes for the isostructural sequence Mg_2SiO_4–Fe_2SiO_4. The new germanate olivine data of our laboratory greatly extend the range of molar volumes (17 per cent) and confirm that the $K_s V_0 = \text{const}$ law applies to this structure as well.

The spinel data in Fig. 13 and Table 8 exhibit considerably greater scatter about a $K_s V_0 = \text{const}$ line, but the data are sufficient to establish the vertical position of the isostructural line for spinels. The single datum for the beta-phase of Mn_2GeO_4 also fits this line which suggests that the spinel and beta phases will have comparable bulk moduli for a given molar volume.

Shankland (1972) and Chung (1972) have derived an equation relating the bulk sound velocity v_ϕ to mean atomic weight $\bar{M}$ from elementary Debye theory of solids:

$$(\partial \ln v_\phi / \partial \ln \bar{M})_X \cong -1/2 \text{ for constant crystallographic structure X;}$$

as this equation relies on the $K_s V_0 = \text{const}$ law for isostructural sequences, it is complementary to the patterns of Fig. 13. The olivine, spinel and beta phase data of Tables 3 and 7 are plotted in a diagram of $\log v_\phi$ against $\log \bar{M}$ in Fig. 14 and the $v_\phi \bar{M}^{\frac{1}{2}}$ scaling law evaluated in Table 8. As with the $K_s - V_0$ results, the olivine and spinel data define systematic $v_\phi \bar{M}^{\frac{1}{2}} = \text{const.}$ trends and the β–Mn_2GeO_4 point fits the spinel sequence. The fit of the data to the isostructural trends in this $v_\phi \bar{M}^{\frac{1}{2}}$ plot is even better than in the $K_s V_0$ diagram (Fig. 13).

A particular noteworthy feature of Figs 13 and 14 and Table 8 is that the germanate, silicate, aluminate and ferrite data may be represented by the same isostructural trends. Similar behaviour has been observed earlier for germanate and silicate compounds with these structures and for the rutile, garnet, ilmenite, and pyroxene structures (Liebermann 1970, 1972a, b, 1973a, c). We conclude that germanate compounds, which have been so important as models of the crystal chemical properties of their silicate analogues, are also useful models for the elastic properties.

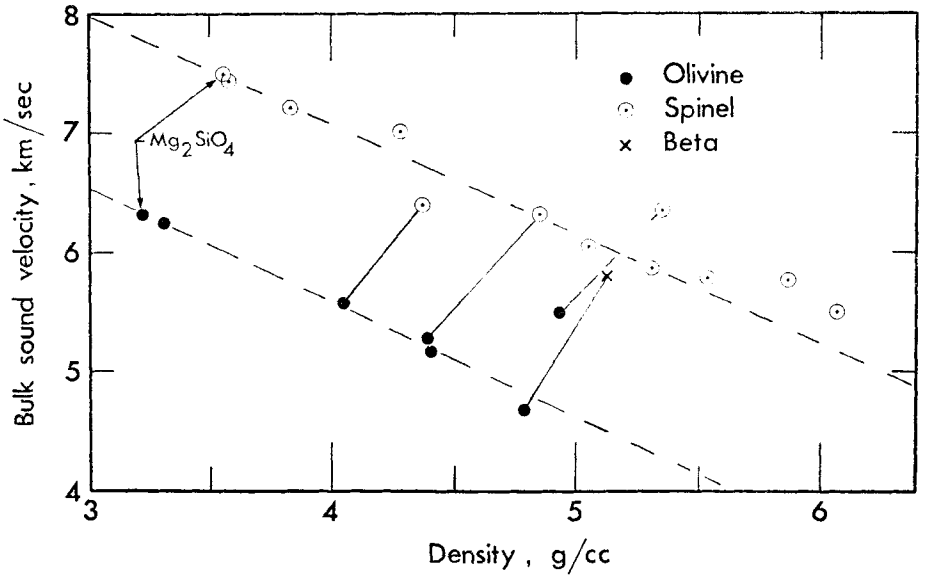

FIG. 15. Bulk sound velocity v_ϕ *vs* density ρ for compounds with olivine, spinel and beta phase structures. Dashed lines connect data for isostructural compounds and are extrapolated to predict $v_\phi = 7{\cdot}5\ \mathrm{km\ s^{-1}}$ for Mg_2SiO_4-spinel ($\rho = 3{\cdot}56\ \mathrm{g\ cm^{-3}}$).

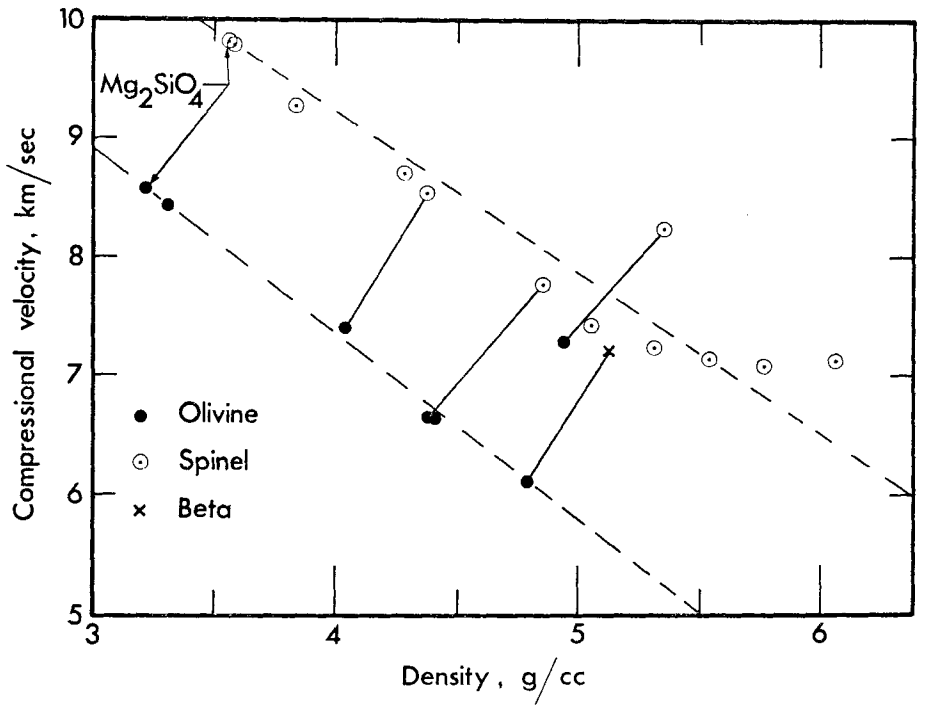

FIG. 16. Compressional velocity v_p *vs* density ρ for compounds with the olivine, spinel and beta phase structures. Dashed lines connect data for isostructural compounds and are extrapolated to predict $v_p = 9{\cdot}8\ \mathrm{km\ s^{-1}}$ for Mg_2SiO_4-spinel ($\rho = 3{\cdot}56\ \mathrm{g\ cm^{-3}}$).

This modelling is applied in Table 9 to predict the elastic properties of Mg_2SiO_4 in the spinel structure. Using the molar volume estimated by Ringwood & Major (1970), both $K_s V_0 = \text{const}$ and $v_\phi M^{-\frac{1}{2}} = \text{const}$ relationships yield comparable estimates of $K_s = 2{\cdot}06 \pm 0{\cdot}05$ Mbar and $v_\phi = 7{\cdot}6 \pm 0{\cdot}1$ km s^{-1}. With only one datum for the beta phase structure, it would be premature to attempt to define trends in Figs 14 and 15. Nevertheless, it is noteworthy that the β–Mn_2GeO_4 values are not significantly different from the spinel patterns.

Birch (1961a) suggested that the compressional velocity v_p decreased linearly with increasing density for minerals with the same crystallographic structure, and others have extended this to describe bulk sound velocity v_ϕ data (McQueen, Fritz & Marsh 1964; Press 1968; Wang 1968b, 1970). Subsequent investigators have verified these suggestions for isomorphic chemical substitutions in the corundum, spinel, olivine, pyroxene, ilmenite and garnet lattices (Liebermann 1970, 1972a, 1973a, 1974; Chung 1970, 1971; Akimoto 1972; Wang & Simmons 1972). Somewhat more regularity in such Birch diagrams has been observed for v_ϕ than for v_p due to the dependence of v_p on the shear modulus, which is sensitive to details of crystallographic structure (Anderson, O. L. & Liebermann 1970; Sammis 1970).

In Figs 15 and 16 we present the data of this paper and other available data in Birch diagrams for v_ϕ and v_p respectively. Systematic patterns are observed for both v_ϕ and v_p for these olivine and spinel compounds. The isostructural trends in Fig. 15 lead to estimates of $v_\phi = 7{\cdot}5$ km s^{-1} for the spinel polymorph of Mg_2SiO_4, in fair agreement with the prediction given in Table 9. This agreement gives us some confidence in estimating compressional velocities from the isostructural trends in Fig. 16; for Mg_2SiO_4, we estimate $v_p = 9{\cdot}8$ km s^{-1} for the spinel forms. This prediction for v_p for the high-pressure polymorph of Mg_2SiO_4 is considerably more tenuous than those of K_s and V_0 in Table 8 but may prove useful until additional evidence is available. Our estimates of the elastic properties of γ–Mg_2SiO_4 are compared with those of previous investigators in Table 10.

In both Figs 15 and 16 we note that the velocities of both the olivine and spinel forms of Ni_2SiO_4 are completely discordant with the trends of their isostructural counterparts. A substantial portion of this deviation from the isostructural trends may be ascribed to the anomalously low molar volumes (and, hence, high densities) of the α and γ polymorphs of Ni_2SiO_4 relative to Mg_2SiO_4 and Fe_2SiO_4 isomorphs (see data in Tables 2 and 9). These anomalous volumes are in turn, a consequence of the fact that Ni^{2+} has the smallest ionic radius in 6-fold co-ordination of the divalent cations, Mg, Ni, Fe, Co (Shannon & Prewitt 1969).

In Fig. 17, Poisson's ratio σ_s is plotted as a function of density ρ. There is a distinct tendency for σ_s to increase as ρ increases as the result of the substitution of heavy metal cations (Fe, Ni, Mn, Co) for Mg in the olivine and spinel structures. Similar behaviour has previously been observed for the α–quartz, zincite, corundum and rocksalt lattices (Anderson, O. L. *et al.* 1968; Liebermann 1972a). We also note

Table 10

Predicted elastic properties at γ–Mg_2SiO_4 ($\rho = 3{\cdot}56$ g/cm^{-3})

	Velocity km s^{-1}			Bulk modulus mbar
	v_p	v_s	v_ϕ	Ks
Mizutani *et al.* (1970)	10·3	—	—	—
Liebermann (1970)	10·03	5·74	7·53	2·01
Chung (1971, 1972)	9·66	5·54	7·24	1·86
Wang & Simmons (1972)	9·73	5·49	7·38	1·94
This paper	(9·8)	(5·4)	7·6	2·06

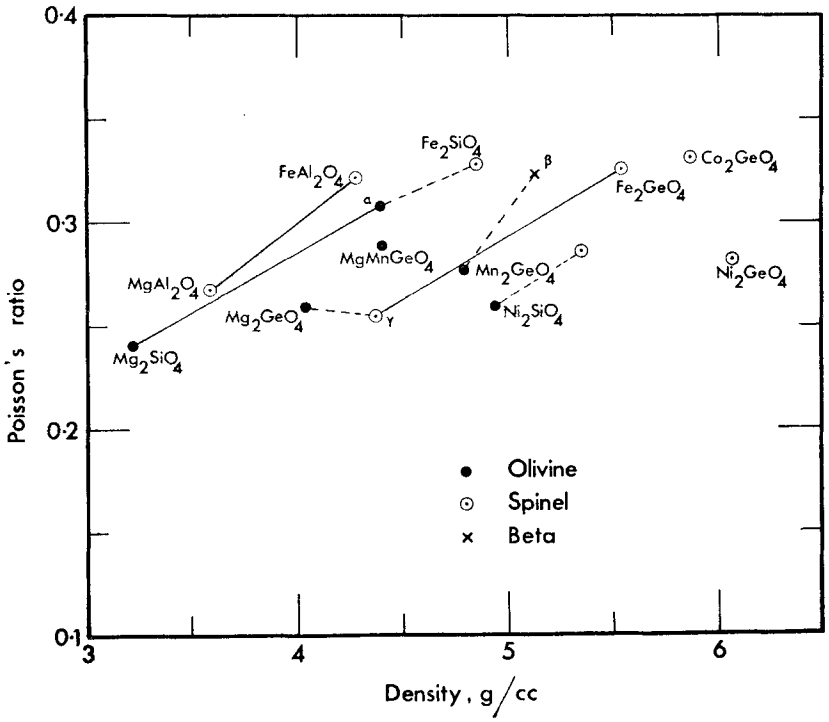

FIG. 17. Poisson's ratio σ_s *vs* density ρ for compounds with the olivine, spinel and beta phase structures. Note tendency for σ_s to increase with ρ as 3*d* transition elements (Fe, Mn, Co, Ni) are substituted for Mg in these germanate and silicate compounds (solid lines). Across polymorphic phase transformations (dashed lines), σ_s remains constant or increases as ρ increases.

here the tendency for σ_s to increase or remain constant across the α–γ and α–β phase transitions, which is no more than a re-statement of the v_p/v_s behaviour demonstrated in Table 4.

4.3 *Comparison of the α–γ and α–β transitions and the 400-km discontinuity in the Earth's mantle*

High-pressure petrological investigations indicate that the primitive upper mantle below the low-velocity zone ($h > 200$ km) is comprised of a complex phase assemblage of olivine, orthopyroxene, clinopyroxene and garnet (Ringwood 1970). Any complete mineralogical interpretation of the transition zone of the Earth's mantle must account for the density and elasticity changes as these upper mantle phases are transformed successively to the more closely-packed crystal structures which characterize the lower mantle, and Ringwood (1970) has constructed a viable model based primarily on crystallographic information for the density changes. Unfortunately, the necessary laboratory elasticity data are not yet available to extend his analysis to a simultaneous interpretation of the observed density and elasticity changes in terms of a complex phase assemblage. In this paper, therefore, we resort to the simplifying assumption that the upper mantle is pure olivine of $(Mg, Fe)_2SiO_4$ composition and reserve the discussion of the more complex, and more realistic, mantle until a future date.

The phase transformation of olivine $(Mg, Fe)_2SiO_4$ to the spinel or β phase structures is now widely accepted as the principal cause of the velocity and density

Table 11

Earth models: Data for density and elastic wave velocities near 400 km depth in mantle.

Model	Depth (km)	ρ g cm^{-3}	v_p (km s^{-1})	v_s (km s^{-1})	v_ϕ (km s^{-1})
Simple Earth[1]	360	3·52	8·71	4·60	6·90
	440	3·87	9·60	5·15	7·54
OC–1[2]	360	3·65	8·65	4·58	6·84
	440	3·86	9·80	5·24	7·71
B1[3]	420	3·58	8·75	4·67	6·90
	420	3·80	9·41	5·32	7·12
1066B[4]	420	3·605	8·893	4·796	6·958
	420	3·746	9·515	5·052	7·515
PEM[5]	420	3·553	8·967	4·806	7·043
	420	3·768	9·554	5·052	7·567

References:

[1] Wang (1972).

[2] Mizutani & Abe (1972).

[3] Jordan (1972); Jordan & Anderson (1974).

[4] Gilbert & Dziewonski (1975).

[5] Dziewonski *et al.* (1975); average Earth model.

discontinuities observed in the Earth's mantle in the neighbourhood of 400 km depth. In an earlier brief report, we compared the experimental laboratory data for the α–β and α–γ transitions with several Earth models in the vicinity of 400 km depth (Liebermann 1973b). The present discussion refines and augments this comparison. Our purpose is to test for consistency between experimental and model data and to suggest possible constraints for future inversion attempts.

We select for this comparison five recent Earth models (Table 11) which are characterized either by first-order discontinuities in velocity and density near 400 km or by regions of anomalously high velocity and density gradients near this depth. In Table 12 we calculate the percentage jumps in density and velocity near 400 km for

Table 12

Earth Models: Density and velocity jumps across 400 km discontinuity

Model	$\Delta\rho$ %	Δv_p %	Δv_s %	Δv_ϕ %	v_p/v_s (change across boundary)
Simple Earth[1]	11	10	12	9	1·89 to 1·86
OC–1[2]	6	13	14	13	1·89 to 1·87
B1[3]	6	8	14	3	1·87 to 1·77
1066B[4]	4	7	5	8	1·85 to 1·88
PEM[5]	6	7	5	7	1·87 to 1·89

References:

[1] Wang (1972).

[2] Mizutani & Abe (1972).

[3] Jordan (1972); Jordan & Anderson (1974).

[4] Gilbert & Dziewonski (1975).

[5] Dziewonski *et al.* (1975).

Table 13

Earth models: Parameters of velocity–density relationships across 400 km discontinuity (for notation see Table 5).

Model	b	λ_p	B	λ_ϕ	n	X
Simple Earth[1]	2·5	1·1	1·8	1·0	0·50	3·0
OC–1[2]	5·5	2·2	4·1	2·1	0·23	5·3
B1[3]	3·0	1·2	1·0	0·5	0·95	2·1
1066B[4]	4·4	1·8	4·0	2·0	0·25	5·0
PEM[5]	2·7	1·1	2·4	1·2	0·41	3·4

References:

[1] Wang (1972).

[2] Mizutani & Abe (1972).

[3] Jordan (1972); Jordan & Anderson (1974).

[4] Gilbert & Dziewonski (1975).

[5] Dziewonski *et al.* (1975).

each of the models. These values should be compared with the experimental data of Table 4, for which the salient features are:

(a) velocity jumps are of comparable percentage magnitude and roughly twice the density change (except for α–β Mn_2GeO_4); and

(b) v_p/v_s ratio is approximately constant or increases across the transitions.

For all of the Earth models except B1 the velocity jumps are of comparable percentage magnitude, but only for OC–1 and 1066B are they twice the density change; it follows directly that all of these four models have v_p/v_s ratios which are approximately constant ($\pm 0{\cdot}03$) across the discontinuity. The B1 model contains an extremely large jump (14 per cent) in v_s at 420 km which greatly exceeds the v_p jump (8 per cent) resulting in a pronounced decrease of v_p/v_s across the discontinuity.

The experimental elasticity data are, of course, appropriate to ambient conditions ($P = 1$ bar, $T = 25\,^\circ$C) whereas the 400 km discontinuity in the mantle probably occurs near $P \approx 125$ kbar and $T \approx 1600\,^\circ$C. Both pressure and temperature cause increases in the ratio v_p/v_s in most minerals (see Anderson, O. L. *et al.* 1968). If we use the olivine (Fo_{93}) data of Kumazawa & Anderson (1969) and the spinel data ($MgO.2.6Al_2O_3$) of Schreiber (1967), the effect of increasing pressure by 125 kbar and temperature by 1600 °C would be to enhance any ambient contrast in v_p/v_s for olivine and spinel by $+0{\cdot}07$.

In Table 13 we calculate the parameters for the various velocity–density relationships discussed in Section 4.1 for the 400 km discontinuities in the Earth models. From the phase transition data in Table 5, we had concluded that $\lambda_\phi{}^P \approx 1{\cdot}7$–$1{\cdot}8$ for the α–γ transition and somewhat larger for α–β Mn_2GeO_4. Of the Earth models, only OC–1 and 1066B are consistent with the laboratory data; note here that since $\lambda_\phi{}^P \approx \lambda_\phi{}^T$ these comparisons remain valid if we correct the ambient elasticity data to mantle conditions. The ' simple Earth ' and PEM models are not compatible with the experimental data and the B1 model is completely discordant.

We conclude from this discussion that only the OC–1 (Mizutani & Abe 1972) and 1066B (Gilbert & Dziewonski 1975) models are consistent with the experimental data for the α–γ and α–β phase transformations in germanate and silicate compounds. Of these two models, 1066B is a more viable model as it has been constrained to satisfy a much larger body of free oscillation data. It is interesting to note that 1066B was derived by perturbing B1 to fit the new data with the requirement that the perturbation added to the starting model be as smooth as possible.

An alternative conclusion is that the experimental data should be used to provide constraints in future inversion attempts to derive geophysical models for the Earth's interior; in particular, the data for the α–γ and α–β phase transformations suggest that at the 400 km discontinuity (1) the velocity jumps for v_p, v_s and v_ϕ should be of comparable percentage magnitude and approximately twice the percentage jump in density (equivalent to $\lambda \approx 2$) and (2) that the v_p/v_s ratio should be constant or increase across the discontinuity. Application of these constraints presupposes, of course, that the olivine–spinel or olivine–beta phase transformations are the cause of the velocity and density discontinuities near 400 km depth in the Earth's mantle.

Acknowledgments

I am grateful to A. E. Ringwood for his continuing encouragement and advice in this collaborative research program. I thank D. J. Mayson and A. Major for preparation of the hot-pressed specimens, and G. F. Davies, A. M. Dziewonski, A. L. Hales and E. R. Lapwood, and F. Gilbert and A. M. Dziewonski for preprints of their papers. I have profited from discussions and a review of the manuscript by A. E. Ringwood, A. L. Hales and L. G. Liu and from an exchange of correspondence with H. Mizutani.

Research School of Earth Sciences,
Australian National University,
Canberra, ACT, Australia.

References

Akimoto, S. I., 1972. The system MgO–FeO–SiO_2 at high pressures and temperatures—phase equilibria and elastic properties, *Tectonophysics*, **13**, 161–187.

Akimoto, S. I., Fujisawa, H. & Katsura, T., 1965. The olivine–spinel transition in Fe_2SO_4 and Ni_2SiO_4, *J. geophys. Res.*, **70**, 1969–1977.

Anderson, D. L., 1967. A seismic equation of state, *Geophys. J. R. astr. Soc.*, **13**, 9–30.

Anderson, D. L. & Anderson, O. L., 1970. Bulk modulus—volume relationship for oxides, *J. geophys. Res.*, **75**, 3494–3500.

Anderson, D. L. & Kanamori, H., 1968. Shock wave equations of state for rocks and minerals, *J. geophys Res.*, **73**, 6477–6502.

Anderson, D. L., Sammis, C. & Jordan, T., 1971. Composition and evolution of the mantle and core. *Science*, **171**, 1103–1112.

Anderson, O. L., 1973. Comments on the power-law representation of "Birch's Law", *J. geophys. Res.*, **78**, 4901–4914.

Anderson. O. L. & Liebermann, R. C., 1970. Eqautions for the pressure derivatives of the elastic constants for three cubic lattices, and some geophysical applications, *Phys. Earth Planet. Int.*, **3**, 61–85.

Anderson, O. L. & Nafe, J. E., 1965. The bulk modulus–volume relationship for oxide compounds and related geophysical problems, *J. geophys. Res.*, **70**, 3951–3963.

Anderson, O. L., Schreiber, E., Liebermann, R. C. & Soga, N., 1968. Some elastic constant data on minerals relevant to geophysics, *Rev. Geophys.*, **6**, 491–524.

Bernal, J. D., 1936. Discussion, *Observatory*, **59**, 268.

Bassett, W. A. & Barnett, J. D., 1970. Isothermal compression of stishovite and coesite up to 85 kilobars at room temperature by X-ray diffraction, *Phys. Earth Planet. Int.*, **3**, 54–60.

Birch, F., 1961a. The velocity of compressional waves in rocks to 10 kilobars, 2, *J. geophys. Res.*, **66,** 2199–2224.

Birch, F., 1961b. Composition of the earth's mantle, *Geophys. J. R. astr. Soc.*, **4,** 295–311.

Birle, J. D., Gibbs, G. V., Moore, P. B. & Smith, J. V., 1968. Crystal structures of natural olivines, *Am. Mineral.*, **53,** 807–824.

Chang, Z. P. & Barsch, G. R., 1973. Pressure dependence of single-crystal elastic constants and anharmonic properties of spinel, *J. geophys. Res.*, **78,** 2418–2433.

Chung, D. H., 1970. Effects of iron/magnesium ratio on P- and S-wave velocities in olivine, *J. geophys. Res.*, **75,** 7353–7361.

Chung, D. H., 1971. Elasticity and equations of state of olivines in the Mg_2SiO_4–Fe_2SiO_4 system, *Geophys. J. R. astr. Soc.*, **24,** 511–538.

Chung, D. H., 1972. Birch's law: why is it so good? *Science*, **177,** 261–263.

Chung, D. H., 1973. Elasticity of high pressure phases (abstract) *EOS*, **54,** 475.

Chung, D. H., 1974. General relationships among sound speeds I. New experimental information, *Phys. Earth Planet. Int.*, **8,** 113–120.

Dachille, F. & Roy, R., 1960. High pressure studies of the system Mg_2GeO_4–Mg_2SiO_4 with special reference to the olivine-spinel transition, *Amer. J. Sci.*, **258,** 225–246.

Davies, G. F., 1974. Elasticity, crystal structure and phase transitions, *Earth Planet. Sci. Lett.*, **22,** 339–346.

Durif-Varambon, E., Bertaut, F. & Pauthenet, R., 1956. Étude des germanates spinels, *Ann. Chim. (Paris)*, **(13) 1,** 525–543.

Dziewonski, A. M., Hales, A. L. & Lapwood, E. R., 1975. Parametrically simple Earth models consistent with geophysical data, *Phys. Earth Planet. Int.*, (Submitted for publication.)

Fang, J. H., Townes, W. D. & Robinson, P. D., 1969. The crystal structure of manganese metagermanate, *Z. Krist.*, **1305,** 139–147.

Gilbert, F. & Dziewonski, A. M., 1975. An application of normal mode theory to the retrieval of structural parameters and source mechanisms from seismic spectra, *Phil. Trans. R. Soc. (Lond.)*. In press.

Graham, E. K. & Barsch, G. R., 1969. Elastic constants of single-crystal forsterite as a function of temperature and pressure, *J. geophys. Res.*, **74,** 5949–5960.

Hales, A. L., 1972. The travel times of P seismic waves and their relevance to the upper mantle velocity distribution, *Tectonophys.*, **13,** 447–482.

Hariya, Y. & Wai, C. M., 1970. The stability and phase transition of the system Fe_2GeO_4–Fe_2SiO_4, *J. Fac. Sci., Hokkaido Univ., Ser.* 4, **14,** 355–363.

Jeffreys, H., 1937. On the materials and density of the earth's crust, *Mon. Not. R. astr. Soc., Geophys. Suppl.*, **4,** 50–61.

Jordan, T. H., 1972. *Estimation of the radial variation of seismic velocities and density in the Earth,* PhD thesis, California Institute of Technology, Pasadena, California.

Jordan, T. H. & Anderson, D. L., 1974. Earth structure from free oscillations and travel times, *Geophys. J. R. astr. Soc.*, **36,** 411–459.

Kamb, B., 1969. Structural basis of the olivine-spinel stability relation, *Amer. Mineral,* **53,** 1439–1453.

Kumazawa, M. & Anderson, O. L., 1969. Elastic moduli, pressure derivatives, and temperature derivatives of single-crystal olivine and single-crystal forsterite *J. geophys. Res.* **74,** 5961–5972.

Liebermann, R. C., 1970. Velocity–density systematics for the olivine and spinel phases of Mg_2SiO_4–Fe_2SiO_4, *J. geophys. Res.*, **75,** 4029–4034.

Liebermann, R. C., 1972a. Elastic properties of minerals determined from ultrasonic or compression data, *Phys. Earth Planet. Int.*, **5,** 312–317.

Liebermann, R. C., 1972b. Compressional velocities of polycrystalline olivine, spinel, and rutile minerals. *Earth Planet. Sci. Letters,* **17,** 263–268.

Liebermann, R. C., 1972c. Pressure and temperature dependence of the elastic properties of polycrystalline trevorite ($NiFe_2O_4$), *Phys. Earth Planet. Int.*, **6**, 360–365.

Liebermann, R. C., 1973a. Elastic properties of germanate analogues of olivine, spinel and β polymorphs of $(Mg,Fe)_2SiO_4$, *Nature Phys. Sci.*, **244**, 105–107.

Liebermann, R. C., 1973b. Elasticity of the olivine-spinel and olivine-β phase transformation and the 400-kilometer discontinuity of the mantle, *J. geophys. Res.*, **78**, 7015–7019.

Liebermann, R. C., 1973c. Elastic properties of polycrystalline SnO_2 and GeO_4: comparison with stishovite and rutile data, *Phys. Earth Planet. Int.*, **7**, 461–465.

Liebermann, R. C., 1974. Elasticity of pyroxene-garnet and pyroxene–ilmenite phase transformations in germanates, *Phys. Earth Planet. Int.*, **8**, 361–374.

Liebermann, R. C. & Ringwood, A. E., 1973. Birch's law and polymorphic phase transformations. *J. geophys. Res.*, **78**, 6926–2932.

Liebermann, R. C. & Ringwood, A. E., 1974a. Elasticity of phase transformations and the iron content of the mantle (abstract), *EOS*, **55**, 416.

Liebermann, R. C. & Ringwood, A. E., 1974b. Elasticity and crystallography of phase transformations (abstract), *EOS*, **56**, 1188.

Liebermann, R. C., Ringwood, A. E., Mayson, D. J., & Major, A., 1975. Hot-pressing of polycrystalline aggregates at very high pressures for ultrasonic measurements, *Proceedings of the 4th International Conference on High Pressure, Kyoto*, Nov 25–29, 1974. The Physico-Chemical Society of Japan, Kyoto.

Liu, L. G., 1970. *Isothermal compression of minerals pertinent to the Earth's mantle*, PhD thesis, University of Rochester, Rochester, New York.

Liu, L. G., Bassett, W. A. & Takahashi, T., 1974. Isothermal compressions of a spinel phase of Co_2SiO_4 and magnesian ilmenite, *J. geophys. Res.*, **79**, 1171–1174.

Mackenzie, J. K., 1950. The elastic constants of a solid containing spherical holes, *Proc. Phys. Soc. London*, **63B**, 2–11.

McQueen, R. G., Fritz, J. N. & Marsh, S. P., 1964. On the composition of the earth's interior, J. *geophys. Res.*, **69**, 2947–2966.

McSkimin, H. J., 1961. Pulse superposition method for measuring ultrasonic wave velocities in solids, *J. acoust. Soc. Am.*, **33**, 12–16.

Mao, H. K., Takahashi, T. & Bassett, W. A., 1970. Isothermal compression of the spinel phase of Ni_2SiO_4 up to 300 kilobars at room temperature, *Phys. Earth Planet. Int.*, **3**, 51–53.

Mao, H. K., Takahashi, T., Bassett, W. A., Weaver, J. S. & Akimoto, S.-I., 1969. Effect of prssure and temperature on the molar volumes of wüstite and of three $(Fe,Mg)_2SiO_4$ spinel solid solutions, *J. geophys. Res.*, **74**, 1061–1069.

Mathur, H. B., Sinha, A. P. B. & Yagnik, C. M., 1965. The Mossbauer spectrum of spinel oxides containing the ferrous ion, *Solid State Comm.*, **3**, 401–403.

Mizutani, H. & Abe, K., 1972. An earth model consistent with free oscillation and surface wave data, *Phys. Earth Planet. Int.*, **5**, 345–356.

Mizutani, H., Hamano, Y. & Akimoto, S. I., 1972. Elastic-wave velocities of polycrystalline stishovite, *J. geophys. Res.*, **77**, 3744–3749.

Mizutani, H., Hamano, Y., Ida, Y, & Akimoto, S. I., 1970. Compressional wave velocities of fayalite, Fe_2SiO_4 spinel, and coesite, *J. geophys. Res.*, **75**, 2741–2747.

Moore, P. B. & Smith, J. V., 1970. Crystal structure of β-Mg_2SiO_4: crystal-chemical and geophysical implications. *Phys. Earth Planet. Int.*, **3**, 166–177.

Morimoto, N., Akimoto, S., Koto, K. & Tokonami, M., 1969. Modified spinel, beta-manganous orthgermanate: stability and crystal structure, *Science*, **165**, 586–588.

Morimoto, N., Tokonami, M. & Koto, K., 1972. Crystal structures of the high pressure polymorphs of Mn_2GeO_4, *Am Mineral.*, **57**, 62–75.

Morimoto, N., Tokonami, M., Watanabe, M. & Koto, K., 1974. Crystal structures of three polymorphs of Co_2SiO_4, *Am. Mineral.*, **59**, 475–485.

Navrotsky, A., 1973. Thermodynamic relations among olivine, spinel, and phenacite structures in silicates and germanates (I) Volume relations and the systems NiO–MgO–GeO_2 and CoO–MgO–GeO_2, *J. Solid State Chem.*, **6,** 21–41.

Navrotsky, A. & Kleppa, O. J., 1968. Thermodynamics of formation of simple spinels, *J. inorg. Nucl. Chem.*, **30,** 479–498.

Press, F., 1968. Earth models obtained by Monte Carlo inversion, *J. geophys. Res.*, **73,** 5223–5234.

Ringwood, A. E., 1958. The constitution of the mantle, II. Further data on the olivine-spinel transition, *Geochim. Cosmochim. Acta*, **15,** 18–29.

Ringwood, A. E., 1962. Prediction and confirmation of olivine-spinel transition in Ni_2SiO_4, *Geochim Cosmochim. Acta*, **26,** 457–469.

Ringwood, A. E., 1970. Phase transformations and the constitution of the mantle, *Phys. Earth Planet. Int.*, **3,** 109–155.

Ringwood, A. E., 1975. *Composition and petrology of the Earth's mantle*, McGraw–Hill, New York.

Ringwood, A. E. & Major, A., 1970. The system Mg_2SiO_4–Fe_2SiO_4 at high pressures and temperatures, *Phys. Earth Planet. Int.*, **3,** 89–108.

Ringwood, A. E. & Reid, A. F., 1970. Olivine–spinel transformation in $MgMnGeO_4$, $FeMnGeO_4$ and $CoMnGeO_4$, *J. Phys. Chem. Solids*, **31,** 2791–2793.

Robie, R. A., Bethke, P. M., Toulmin, M. S. & Edwards, J. L., 1966. X-ray crystallographic data, densities, and molar volumes of minerals, *Handbook of Physical Constants*, Section 5, pp. 27–73, Revised Edition, ed. S. P. Clark, Geological Society of America, *Memoir* 97, New York.

Sammis, C. G., 1970. The pressure dependence of the elastic constants of cubic crystals in the NaCl and spinel structures from a lattice model, *Geophys. J. R. astr. Soc.*, **19,** 285–297.

Schreiber, E., 1967. Elastic moduli of single crystal spinel at 25°C and to 2 kbar, *J. appl. Phys.*, **38,** 2508–2511.

Shankland, T. J., 1972. Velocity–density systematics: derivation from Debye theory and the effect of ionic size, *J. geophys. Res.*, **77,** 3750–3758.

Shankland, T. J. & Chung, D. H., 1974. General relationships among sound speeds II. Theory and discussion, *Phys. Earth Planet. Int.*, **8,** 121–129.

Shannon, R. D. & Prewitt, C. T., 1969. Effective ionic radii in oxides and fluorides, *Acta Cryst.*, **B25,** 925–945.

Shaw, G., 1974. Phase transitions, elasticity-density relations, and the univalent halides, *J. geophys. Res.*, **79,** 2635–2643.

Simmons, G. & England, A. W., 1969. Universal equations of state for oxides and silicates, *Phys. Earth Planet. Int.*, **2,** 69–76.

Smith, G. S. & Alexander, L. E., 1963. Refinement of the atomic parameters of α-quartz, *Acta Cryst.*, **16,** 426–471.

Smith, G. S. & Isaacs, P. B., 1964. The crystal structure of quartz-like GeO_2, *Acta Cryst.*, **17,** 842–846.

Soga, N., 1971. Sound velocity of some germanate compounds and its relation to the law of corresponding states, *J. geophys. Res.*, **76,** 3983–3989.

Spetzler, H., 1970. Equation of state of polycrystalline and single crystal MgO to 8 kilobars and 800°K, *J. geophys. Res.*, **75,** 2073–2087.

Wang, C. Y., 1968a. Equation of state of periclase and Birch's relationship between velocity and density, *Nature (Lond.)*, **218,** 74–76.

Wang, C. Y., 1968b. Constitution of the lower mantle as evidenced from shock-wave data for some rocks, *J. geophys. Res.*, **73,** 6459–6476.

Wang, C. Y., 1969. Equation of state of periclase and some of its geophysical implications, *J. geophys. Res.*, **74,** 1451–1457.

Wang, C. Y., 1970. Density and the constitution of the mantle, *J. geophys. Res.*, **75,** 3264–3284.

Wang, C. Y., 1972. A simple earth model, *J. geophys. Res.*, **77,** 4318–4329.
Wang, H. & Simmons, G., 1972. Elasticity of some mantle crystal structures. I. Pleonaste and hercynite spinel, *J. geophys. Res.*, **77,** 4379–4392.
Yagi, T., Marumo, F. & Akimoto, S. I., 1974. Crystal structures of spinel polymorph of Fe_2SiO_4 and Ni_2SiO_4, *Am. Mineral.*, **59,** 486–490.
Zoltai, T. & Buerger, M. J., 1959. The crystal structure of coesite, the dense, high-pressure form of silica, *Z. Krist.*, **111S,** 129–141.